Chapter 4. Zwitterionic and cationic bis(phosphine) platinum(II) complexes: comparative studies relevant to ligand exchange and benzene C-H activation processes

The text of this chapter is reproduced in part with permission from:

Thomas, J. C.; Peters, J. C. *J. Am. Chem. Soc.* **2003**, *125*, 8870-8888.

4.1. Introduction

Organometallic cations are ubiquitous in homogeneous catalysis, with applications spanning catalytic C-E bond forming reactions (E = H, C, Si), polymerizations, and alkane activation processes.[1,2] Our group is exploring the chemistry of neutral, formally zwitterionic complexes that are related to reactive organometallic cations supported by conventional phosphine and amine donors.[3] These neutral complexes are characterized by (phosphino)- and (amino)borate ligands in which a borate unit is contained within the ligand backbone, partially insulated from the coordinated metal center, so as to preserve reactivity associated with their cationic relatives. Zwitterionic systems of this type may ultimately complement their cationic cousins by virtue of (i) their solubility and high activity in less polar, non-coordinating solvents, (ii) their potential to show increased tolerance to polar or coordinating functional groups that one might expect to attenuate the reactivity of cationic systems, and (iii) the attenuation of counterion effects which may be present in discrete salt systems.

To begin evaluating this approach to catalysis, it needs to be established whether these neutral systems will give rise to reaction profiles similar to those traditionally associated with their cationic analogues. Many factors are likely to impact this issue: in particular, it is possible that a borate counter-anion rigidly fastened in close proximity to a coordinated metal center will alter the complex's overall reactivity and the operational mechanism by which it mediates a reaction transformation to some extent. Therefore, it was of interest to study how the mechanisms of electronically distinct but structurally related neutral and cationic systems compare for a shared organometallic reaction process. Little attention has been devoted to such issues previously.[4] In this chapter, we examine the kinetic and mechanistic profiles of structurally related neutral and cationic

platinum(II) systems that each mediate an elementary C-H bond activation process in benzene solution.

In light of the intense interest in electrophilic C-H activation reactions mediated by late transition metal centers,[5-13] a C-H activation study that compares a neutral with a cationic system is timely. Three platinum(II) systems supported by the structurally related, bidentate phosphine ligands, [Ph_2BP_2] (**2.25**), Ph_2SiP_2 (**3.22**), and dppp (**3.23**), are featured (Figure 4.1). The major structural difference between complexes supported by **2.25**, **3.22**, and **3.23** is in the ligand backbone, relatively removed from the phosphine-coordinated metal center. Ligand **2.25** contains an anionic borate unit that, when bound to a $Pt^{II}(X)(L)$ species, affords a neutral and formally zwitterionic [Ph_2BP_2]Pt(X)(L) complex. In this neutral system, the anion is structurally contained within the ligand framework at a distance of approximately 4 Å from the coordinated platinum center in the solid state. Ligand **3.22** replaces the diphenylborate unit of **2.25** with a structurally similar diphenylsilane unit, and ligand **3.23** contains the more common methylene backbone. Systems supported by **3.22** and **3.23** provide access to more conventional cationic species of the type $[P_2Pt^{II}(X)(L)][X']$, where the primary difference is that, in solution, the counter-anion is at an ill-defined distance from the coordinated platinum center with the potential to ion-pair with the metal center.

Because a methyl solvento complex of each ligand system proved capable of mediating an elementary benzene C-H bond activation process (Figure 4.1), the three systems provided an opportunity for a comparative mechanistic study. Herein, we provide spectroscopic and kinetic information for the phosphine-supported neutral and cationic platinum(II) systems. These data are considered with respect to the mechanistic

profile of each system in benzene solution. Specifically, we highlight several important and unexpected mechanistic distinctions between the systems.

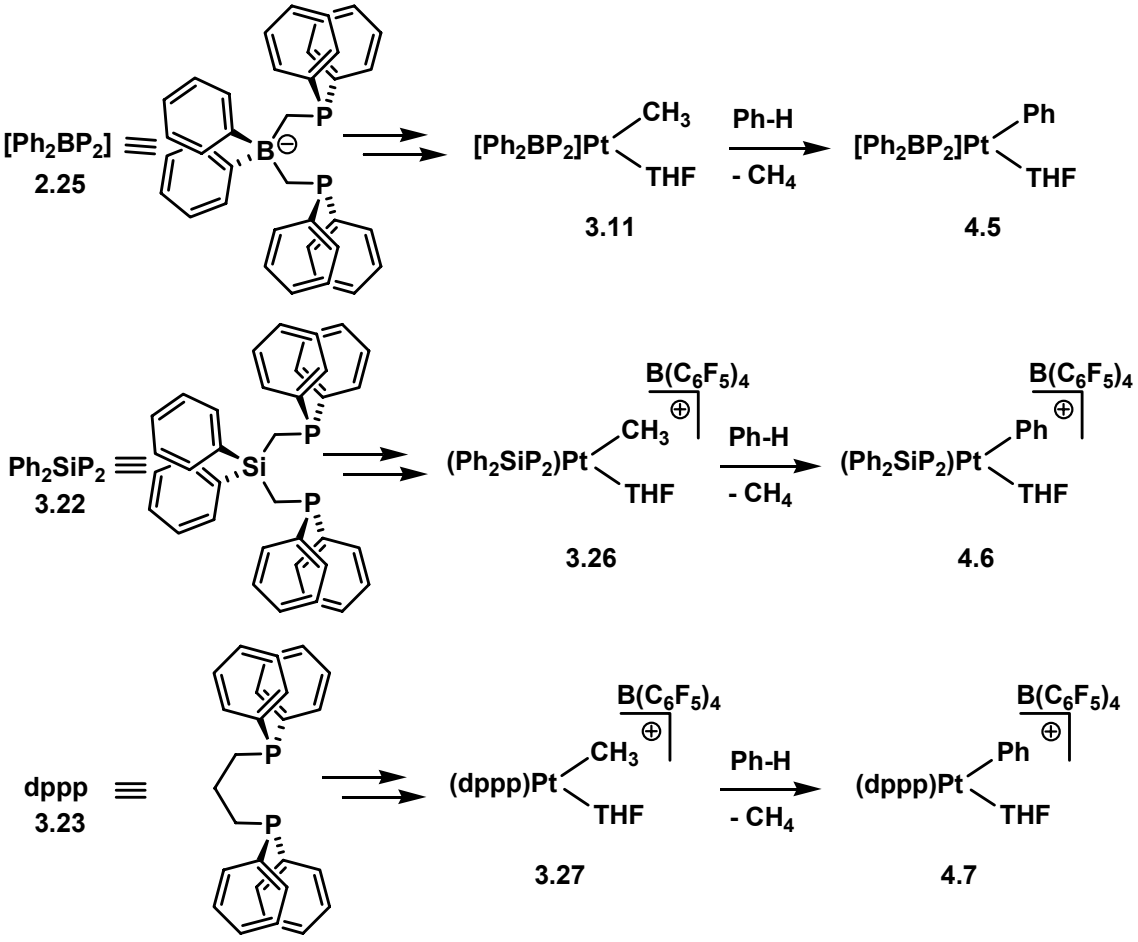

Figure 4.1. Labeling scheme for the phosphine ligands featured in this chapter and the model benzene C-H activation reaction used for the comparative study.

4.2. Results and discussion

4.2.1. Syntheses of methyl solvento and phenyl solvento complexes

The key complexes for the comparative C-H activation study were the methyl THF complexes $[Ph_2BP_2]Pt(Me)(THF)$ (**3.11**), $[(Ph_2SiP_2)Pt(Me)(THF)][B(C_6F_5)_4]$ (**3.26**), and $[(dppp)Pt(Me)(THF)][B(C_6F_5)_4]$ (**3.27**). The syntheses of these compounds are described in Chapter 3. For studies relevant to the mechanistic interpretation, we also prepared the d_{20}-$[Ph_2BP_2]$ ligand $[Ph_2B(CH_2P(C_6D_5)_2)_2]$ according to eq 4.1. Although

d_{10}-methyldiphenylphosphine was synthesized in very pure form with virtually no detectable aryl protons (^{1}H NMR), subsequent lithiation followed by addition of diphenylchloroborane to form the required borate ligand gave rise to a small degree (less than 10%) of proton incorporation in the phosphine phenyl rings. Neutral $[Ph_2B(CH_2P(C_6D_5)_2)_2]Pt(Me)(THF)$ (**3.11-*d*$_{20}$**) was subsequently synthesized in a manner identical to the preparation of **3.11**. The structural comparison of **3.1**, **3.24**, and **3.25** presented in the previous chapter suggests that these systems provide structurally analogous compounds; however, spectroscopic measurements imply that complexes supported by the anionic $[Ph_2BP_2]$ ligand may be described as more electron-rich at the metal center.

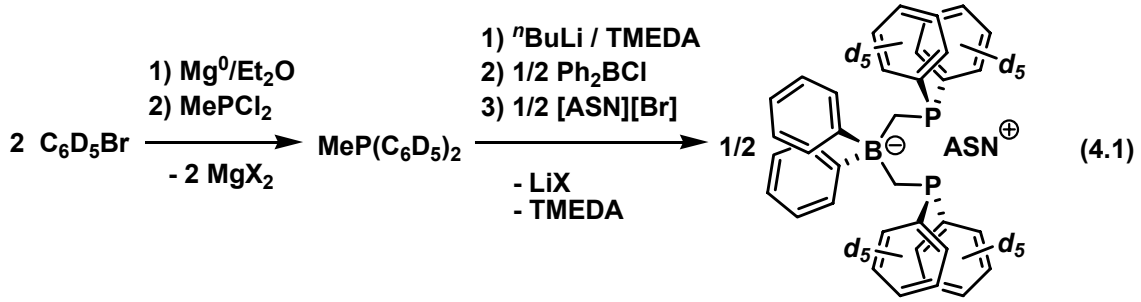

To provide spectroscopic guides for studying the benzene C-H activation process, we independently prepared and characterized the corresponding phenyl derivatives $[Ph_2BP_2]Pt(Ph)(THF)$ (**4.5**), $[(Ph_2SiP_2)Pt(Ph)(THF)][B(C_6F_5)_4]$ (**4.6**), and $[(dppp)Pt(Ph)(THF)][B(C_6F_5)_4]$ (**4.7**). Neutral **4.5** was prepared by two independent routes: either abstraction of a methyl ligand from $[[Ph_2BP_2]Pt(Me)(Ph)][ASN]$ (**4.1**) using the strong Lewis acid $B(C_6F_5)_3$ (eq 4.2) or by protonation of the diphenyl complex $[[Ph_2BP_2]Pt(Ph)_2][ASN]$ (**4.2**) using $[^iPr_2EtNH][BPh_4]$ (eq 4.3). Neutral **4.5** was characterized fully by NMR spectroscopy for both routes, but isolating analytically pure material was compromised by difficulties in separation and the lability of the solvent

THF molecule. Compounds **4.6** and **4.7** were generated cleanly by protonation of the corresponding diphenyl compounds $(Ph_2SiP_2)PtPh_2$ (**4.3**) and $(dppp)PtPh_2$[14] (**4.4**) with $[H(OEt_2)_2][B(C_6F_5)_4]$[15] in dichloromethane in the presence of approximately 40 to 100 equivalents of THF (eq 4.4). The phenyl derivatives **4.5**, **4.6**, and **4.7** proved less thermally stable than their corresponding methyl analogues (*vide infra*).

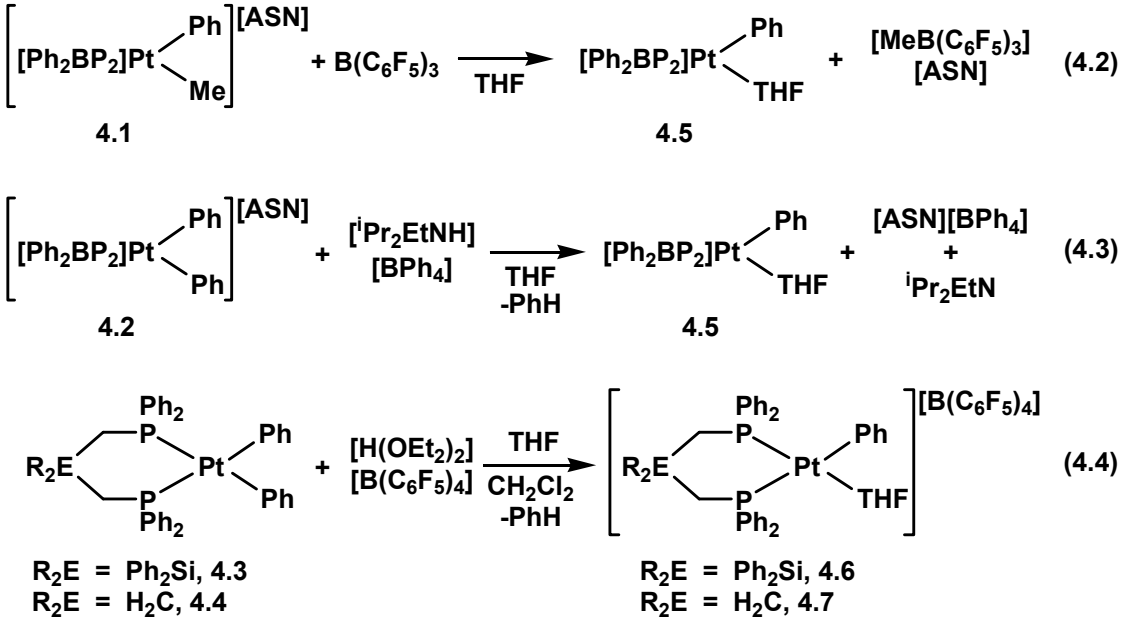

4.2.2. Determination of relative THF ligand exchange rates for 3.11 and 3.26

The relative rates and mechanisms of ligand exchange in benzene solution are important to mechanistic considerations discussed in subsequent sections. Measurement of the rate of THF self-exchange for $[Ph_2BP_2]Pt(Me)(THF)$ (**3.11**) and $[(Ph_2SiP_2)Pt(Me)(THF)]^+$ (**3.26**) was therefore examined in benzene-d_6 in the presence of excess THF through the NMR technique of magnetization transfer using a DANTE pulse sequence[16] (eq 4.5 and eq 4.6). Saturation of the free downfield THF resonance near 3.6 ppm transferred intensity to the downfield platinum-bound THF resonance near 2.9 ppm in each case, and the rate constant for THF exchange (k_{ex}) was extracted from the NMR

data using the computer program CIFIT.[17] Attempts to determine rates of THF self-exchange for $[(dppp)Pt(Me)(THF)]^+$ (**3.27**) were unsuccessful due to poor fitting of the data by CIFIT.

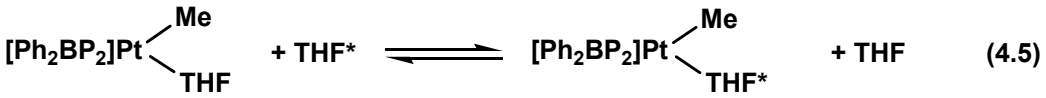

(4.5)

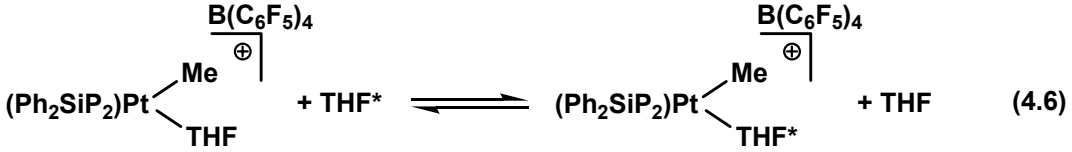

(4.6)

The dependence of the observed rate constant k_{ex} on the concentration of THF was surprisingly different between the neutral and cationic platinum systems. For neutral $[Ph_2BP_2]Pt(Me)(THF)$ (**3.11**), k_{ex} showed no [THF] dependence over a range of THF concentration (0.146 to 0.468 M). In contrast, cationic $[(Ph_2SiP_2)Pt(Me)(THF)]^+$ (**3.26**) showed a first-order dependence on [THF] (0.0766 to 0.237 M) for the observed rate constant (Figure 4.2a). The extrapolated intercept for the plot of k_{ex} versus THF equivalents for **3.26** intersects at the origin and thereby suggests negligible mechanistic dependence on the solvent (benzene) and/or the $[B(C_6F_5)_4]$ anion.[18] The results of these THF dependence studies provided the rate expressions shown in eq 4.7 and eq 4.8, where k_{ex}(**3.11**) = k_B and k_{ex}(**3.26**) = k_{Si}[THF].

$$\textit{rate} = k_B[3.11] \qquad (4.7)$$

$$\textit{rate} = k_{Si}[3.26][THF] \qquad (4.8)$$

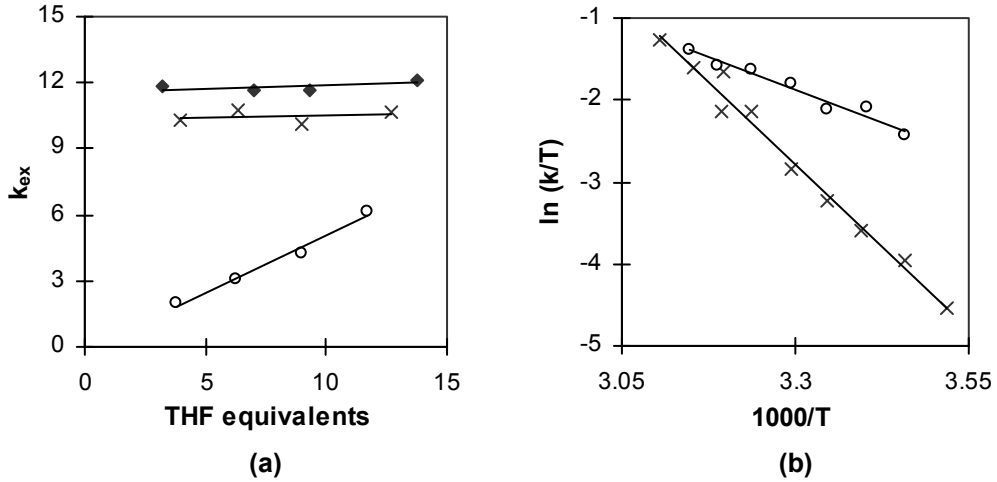

Figure 4.2. (a) Plot of k_{ex} versus THF equivalents for $[Ph_2BP_2]Pt(Me)(THF)$ (**3.11**, ×), $[Ph_2B(CH_2P(C_6D_5)_2)_2]Pt(Me)(THF)$ (**3.11-*d*$_{20}$**, ♦), and $[(Ph_2SiP_2)Pt(Me)(THF)]^+$ (**3.26**, o). (b) Eyring plot of $ln(k_B/T)$ versus 1000/T for neutral methyl solvento complex **3.11** (×) and $ln(k_{Si}/T)$ versus 1000/T cationic methyl solvento complex **3.26** (o).

The absolute difference in the observed rate constant of THF self-exchange (k_B, k_{Si}) at a given temperature between complex $[Ph_2BP_2]Pt(Me)(THF)$ (**3.11**) and $[(Ph_2SiP_2)Pt(Me)(THF)]^+$ (**3.26**) is modest. For example, at 25 °C, the rate constant for neutral **3.11** ($k_{B(298K)}$(**3.11**) = 12.0 s^{-1}) is approximately one third as large as that for cationic **3.26** ($k_{Si(298K)}$(**3.26**) = 38.5 M^{-1} s^{-1}). More interesting is that the temperature dependence of k_B and k_{Si} is significantly different between **3.11** and **3.26**. The rate constant k_B of $[Ph_2BP_2]Pt(Me)(THF)$ (**3.11**) was examined over the temperature range 11.2-48.9 ºC and provided an entropy and enthalpy of activation as follows: $\Delta S^{\ddagger}_{298K}$ = 0.1 ± 5.4 e.u.; $\Delta H^{\ddagger}$ = 16.0 ± 1.6 kcal/mol (Figure 4.2b). Analogous data collected for cationic $[(Ph_2SiP_2)Pt(Me)(THF)]^+$ (**3.26**) over the temperature range 16.0-44.6 ºC provided distinctly different values: $\Delta S^{\ddagger}_{298K}$ = -30.2 ± 5.2 e.u. and $\Delta H^{\ddagger}$ = 1.9 ± 0.5 kcal/mol (Figure 4.2b).

The activation parameters obtained for $[(Ph_2SiP_2)Pt(Me)(THF)]^+$ (**3.26**) ($\Delta S^{\ddagger}_{298K}$ = -30.2 ± 5.2 e.u.; $\Delta H^{\ddagger}$ = 1.9 ± 0.5 kcal/mol) are consistent with an associative mechanism of ligand exchange (eq 4.9), in accord with the first-order dependence of the exchange rate constant on THF concentration. Associative ligand exchange is common for ligand substitution in square planar platinum(II) systems and is the mechanism we had anticipated for **3.26**. Particularly noteworthy is that $\Delta H^{\ddagger}$ for **3.26** suggests that THF exchange is a nearly thermoneutral process – the degree of Pt-O bond making and bond breaking being symmetric in the transition state.

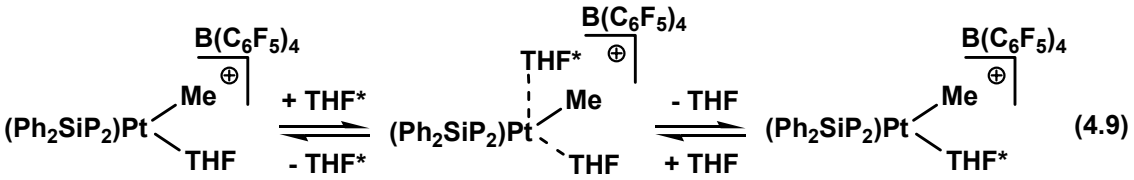

(4.9)

Interpreting the activation parameters and lack of [THF] dependence on k_{ex} of $[Ph_2BP_2]Pt(Me)(THF)$ (**3.11**) is less straightforward. The difference in $\Delta H^{\ddagger}$ between **3.11** and $[(Ph_2SiP_2)Pt(Me)(THF)]^+$ (**3.26**) reflects a change in mechanism, which could include an energy barrier for significant THF dissociation, or association of a more hindered ligand to displace THF. Perhaps the simplest ligand exchange scenario is a purely dissociative mechanism that proceeds via a neutral three-coordinate intermediate, "$[Ph_2BP_2]Pt(Me)$" (eq 4.10). If the platinum center in $[Ph_2BP_2]Pt(Me)(THF)$ (**3.11**) is more electron-rich relative to $[(Ph_2SiP_2)Pt(Me)(THF)]^+$ (**3.26**), dissociation of a σ-donor ligand might be expected to be more favorable. However, simple dissociative exchange mechanisms are rarely observed in platinum(II) substitution chemistry.[19a] Even in cases where they have been reported, such as the systems examined by Romeo,[19] certain assumptions are required to suggest the presence of a three-coordinate intermediate

species. Therefore, two additional mechanisms for THF exchange in $[Ph_2BP_2]Pt(Me)(THF)$ (**3.11**) need also to be considered: solvolytic displacement of the bound THF from **3.11** by benzene itself (eq 4.11) and an anchimeric mechanism whereby a bond pair from the ancillary $[Ph_2BP_2]$ ligand coordinates the platinum center prior to appreciable Pt-O bond breaking (eq 4.12). These latter two possibilities constitute associative interchange mechanisms involving discrete five-coordinate, rather than three-coordinate, intermediates. While we cannot distinguish between dissociative, solvent-assisted, or ligand-assisted exchange pathways from the exchange data alone, the solution NMR data that are discussed below suggest that an anchimeric pathway for ligand exchange is most likely operative for neutral $[Ph_2BP_2]Pt(Me)(THF)$ (**3.11**).

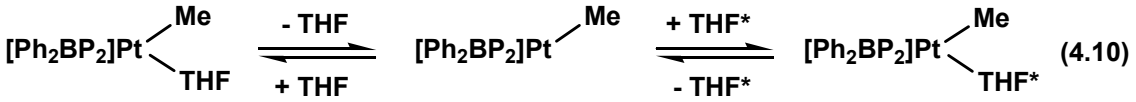

(4.10)

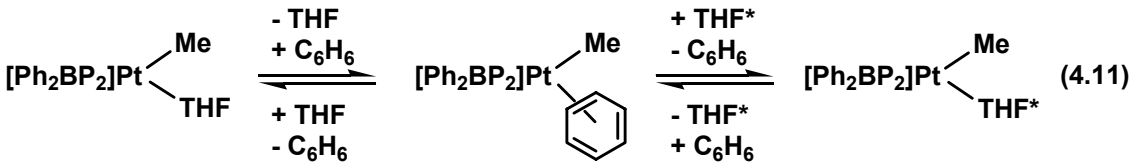

(4.11)

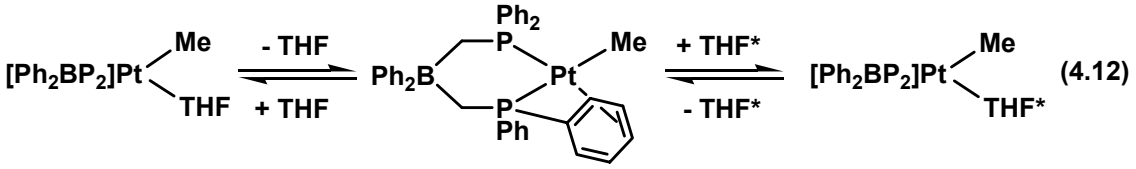

(4.12)

To probe for the possibility of an isotope-dependent change in the rate of THF self-exchange for neutral $[Ph_2BP_2]Pt(Me)(THF)$ (**3.11**), we also investigated the d_{20}-labeled complex $[Ph_2B(CH_2P(C_6D_5)_2)_2]Pt(Me)(THF)$ (**3.11-*d*$_{20}$**). The [THF] dependence of k_{ex} for THF self-exchange for **3.11-*d*$_{20}$** was determined at several THF concentrations (0.116 – 0.497 M) and was found to be independent of [THF] (Figure 4.2a). The observed rate constant, k_{ex}(**3.11-*d*$_{20}$**) = 11.6 ± 0.9 s^{-1} was similar in magnitude

to that measured for $[Ph_2BP_2]Pt(Me)(THF)$ (**3.11**) under similar conditions (k_{ex}(**3.11**) = $10.3 \pm 2.1\ s^{-1}$).

4.2.3. Bond activation reaction pathways of methyl solvento complexes 3.11, 3.26, and 3.27

Zwitterionic $[Ph_2BP_2]Pt(Me)(THF)$ (**3.11**) was initially prepared to examine its bond activation chemistry due to the presence of the highly labile THF ligand. During the course of these investigations, it was found that **3.11** reacts with a variety of E-H bonds, including H-H, Si-H, B-H, and aryl C-H bonds. We initially reported that $[Ph_2BP_2]Pt(Me)(THF)$ (**3.11**) reacts in benzene solution at 50 °C over a period of several hours to form $[Ph_2BP_2]Pt(Ph)(THF)$ (**4.5**) as the major product (approximately 80%) with concomitant liberation of methane.[3a] This reaction requires both heating and an absence of additional equivalents of THF to proceed at reasonable rate (hours). In contrast, **3.11** reacts rapidly (minutes) in THF solution with triethylsilane, pinacolborane, and dihydrogen at ambient temperature. These results suggest that the rate of the reaction may be controlled by the donating ability of the substrate and/or the barrier to E-H bond activation. An additional note is that the products of the bond activation differ between benzene and these other substrates. Benzene reacts cleanly to form a new Pt-C bond, eliminating a C-H bond in the process. Triethylsilane, pinacolborane, and dihydrogen all react to quantitatively form a Pt-H bond and eliminate the E-C bond instead (Figure 4.3). The resulting product is a hydride-bridged platinum(II) dimer, $\{[Ph_2BP_2]Pt(\mu\text{-}H)\}_2$ (**4.8**). The dimer **4.8** has been thoroughly characterized, and its molecular structure was obtained through an X-ray diffraction study (Figure 4.4). Despite being the only product of several E-H bond activation processes, **4.8** has never observed in benzene C-H activation reactions.

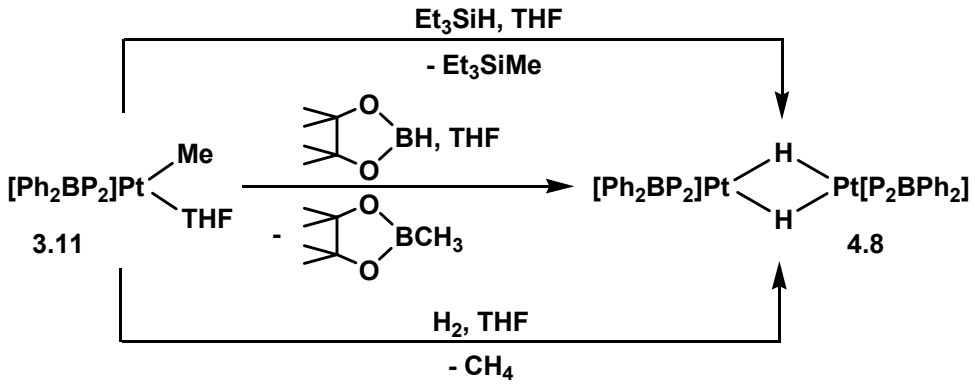

Figure 4.3. Reaction of zwitterionic **3.11** with E-H bonds (E = H, Si, B).

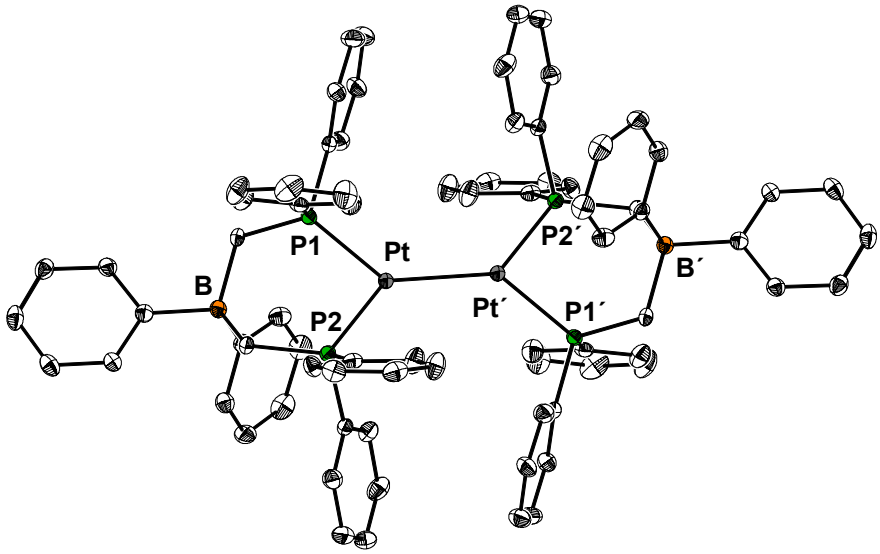

Figure 4.4. Displacement ellipsoid representation (50%) of $\{[Ph_2BP_2]Pt(\mu\text{-}H)\}_2$ (**4.8**). Hydrogen atoms are omitted for clarity. Selected interatomic distances (Å) and angles (º): Pt-P1, 2.241(1); Pt-P2, 2.256(1); Pt-Pt´, 2.6124(5); Pt-B, 3.787(4); P2-Pt-P1, 88.04(3); P1-Pt-Pt´, 136.39(3); P2-Pt-Pt´, 135.23(2).

The cationic derivatives $[(Ph_2SiP_2)Pt(Me)(THF)]^+$ (**3.26**) and $[(dppp)Pt(Me)(THF)]^+$ (**3.27**) were also examined with respect to benzene C-H activation. Both cations reacted to liberate methane upon thermolysis in benzene and to produce the corresponding phenyl derivatives $[(Ph_2SiP_2)Pt(Ph)(THF)]^+$ (**4.6**) and $[(dppp)Pt(Ph)(THF)]^+$ (**4.7**) (Figure 4.1). Neither zwitterionic **4.5** nor the cationic phenyl

complexes **4.6** or **4.7** were stable to extended thermolysis, as demonstrated by the growth of new resonances in their respective $^{31}P\{^{1}H\}$ NMR spectra. Cationic phenyl complexes **4.6** and **4.7** each gave rise to quantitative formation of a single new product (eq 4.13, eq 4.14). Spectroscopic and structural evidence (Figure 4.5) established the products formed to be the orange dinuclear species $[\{(Ph_2SiP_2)Pt\}_2(\mu\text{-}\eta^3\text{:}\eta^3\text{-biphenyl})][B(C_6F_5)_4]_2$ (**4.9**) and $[\{(dppp)Pt\}_2(\mu\text{-}\eta^3\text{:}\eta^3\text{-biphenyl})][B(C_6F_5)_4]_2$ (**4.10**), the apparent products of a bimolecular aryl coupling process. It is noted that the addition of excess THF significantly inhibited the degradation of pure samples of **4.5**-**4.7** in benzene solution. Whereas complex **4.9** proved relatively stable to hydrolysis, complex **4.10** is quite moisture sensitive. The product of hydrolysis of **4.10** is most likely $[\{(dppp)Pt(\mu\text{-}OH)\}_2][B(C_6F_5)_4]_2$, based on the presence of a single new resonance in the $^{31}P\{^{1}H\}$ NMR spectrum which is consistent with a dimeric platinum complex. During the course of this study, Konze, Scott, and Kubas reported a related coupling reaction for similar cationic bisphosphine platinum(II) complexes; however, the aryl intermediates that presumably result from C-H bond activation processes were not observed. The resulting bridged biaryl complexes obtained by Konze *et al.* displayed significant moisture sensitivity, similar to **4.10**, producing bridged μ-OH platinum dimers. We presume that a common mechanism for aryl coupling is active in all of these systems, but that the subtle differences in the bisphosphine ligands give rise to different reaction rates for the steps converting the mononuclear phenyl species to their bridged biphenyl products and the subsequent hydrolysis of the biaryl complex.

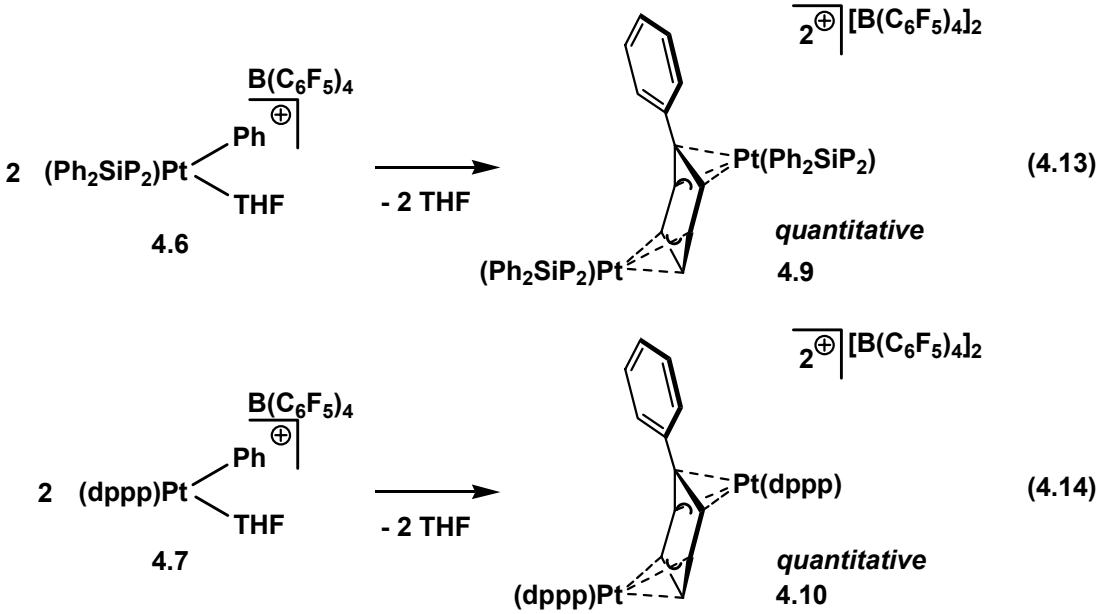

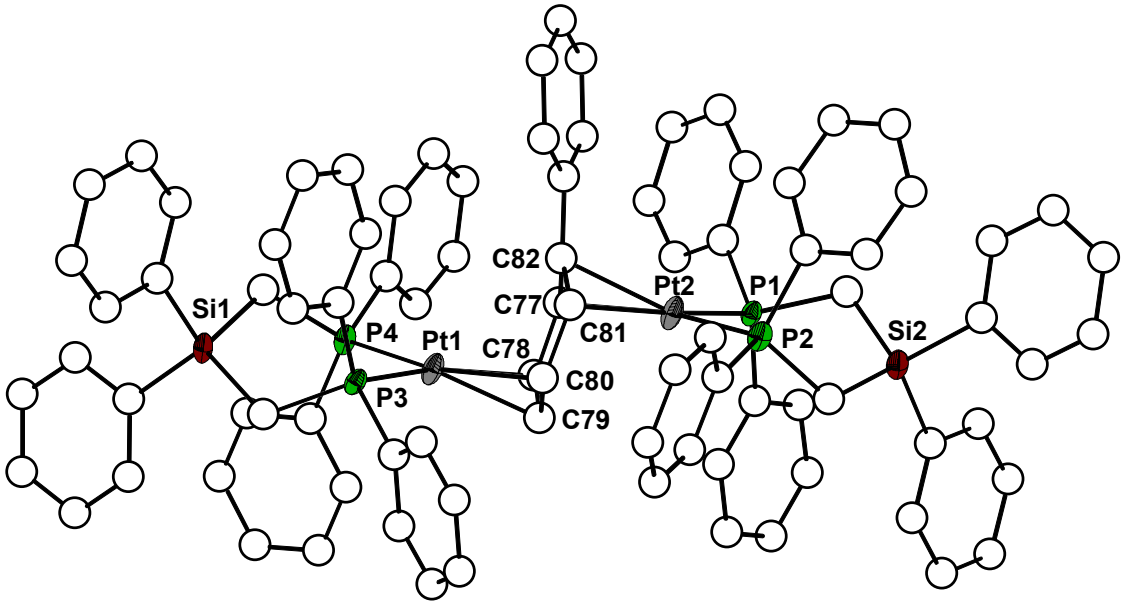

Figure 4.5. Structural representation of [{$(Ph_2SiP_2)Pt$}$_2$(μ-η^3:η^3-biphenyl)][$B(C_6F_5)_4$]$_2$·4(*o*-xylene) (**4.9·4(*o*-xylene)**). Silicon, phosphorus, and platinum atoms are represented by 50% displacement ellipsoids. All carbon atoms were solved isotropically. Hydrogen atoms, [$B(C_6F_5)_4$] anions, and *o*-xylene molecules are omitted for clarity.

Prolonged thermolysis of an independently prepared sample of [Ph_2BP_2]Pt(Ph)(THF) (**4.5**) resulted in two apparent reaction pathways (eq 4.15). The

dominant pathway was that of disproportionation to generate the colorless molecular salt $\{[Ph_2BP_2]Pt(Ph)_2\}^-\{[Ph_2BP_2]Pt(THF)_2\}^+$. Formation of this cation/anion pair was suggested by the appearance of two singlets ($^{31}P\{^1H\}$ NMR) in a 1:1 ratio, and by a positive identification of each ion by electrospray mass spectroscopy. Additionally, the species $[[Ph_2BP_2]Pt(Ph)_2][ASN]$ (**4.2**) was independently prepared and characterized. A small amount of a presumed bridged-biphenyl species was also evident by $^{31}P\{^1H\}$ NMR spectroscopy and by the orange solution color that developed upon prolonged thermolysis. An independent X-ray diffraction study on crystals of this minor species obtained by fractional crystallization provided connectivity consistent with the dinuclear complex $\{[Ph_2BP_2]Pt\}_2(\mu\text{-}\eta^3\text{:}\eta^3\text{-biphenyl})$.

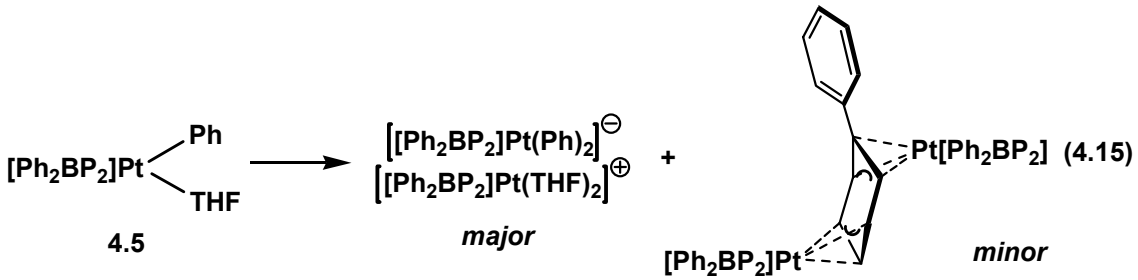

4.2.4. Benzene C-H bond activation kinetics for 3.11, 3.26, and 3.27

To evaluate the benzene C-H bond reactivity of the methyl solvento systems $[Ph_2BP_2]Pt(Me)(THF)$ (**3.11**), $[(Ph_2SiP_2)Pt(Me)(THF)]^+$ (**3.26**), and $[(dppp)Pt(Me)(THF)]^+$ (**3.27**), reaction rates were measured under comparative conditions by monitoring the decay of the starting precursors **3.11**, **3.26**, and **3.27** by either $^{31}P\{^1H\}$ or ^1H NMR spectroscopy. The observed rate constants and half-lives are summarized in Table 4.1, and relevant first-order plots are presented in Figure 4.6 and Figure 4.7.

Table 4.1. Kinetic rate data fit to a first-order decay of **3.11**, **3.26**, and **3.27**.

Complex	Solvent	Temp (ºC)	Additive	Rate (x 10^{-4} s^{-1}) [a]	$t_{1/2}$ (min)
3.11	C_6H_6	45	-	1.42(5)	81
	C_6D_6	45	-	1.13(3)	102
	C_6H_6	45	5 equiv. THF	0.090(3)	1280
	C_6H_6	45	1 equiv. [^{n}Bu$_4$N][B(C_6F_5)$_4$]	1.37(3)	84
	C_6D_6	55	-	3.7(2)	31
	C_6H_6	55	5 equiv. THF	3.18(11)	360
3.26	C_6H_6	55	-	1.80(6)	64
	C_6D_6	55	-	0.276(7)	430
	C_6H_6	55	5 equiv. THF	0.060(6)	1900
	C_6H_6	55	1 equiv. [^{n}Bu$_4$N][B(C_6F_5)$_4$]	1.34(3)	86
3.27	C_6H_6	55	-	≥1.8	≤65
	C_6D_6	55	-	≥0.30	≤400
	C_6H_6	55	5 equiv. THF	0.042(4)	2700

[a] Rates are reported as the average of three trials and errors are reported as the standard deviation.

Both [Ph_2BP_2]Pt(Me)(THF) (**3.11**) and [(Ph_2SiP_2)Pt(Me)(THF)]$^+$ (**3.26**) displayed clean first-order decay at 45 °C and 55 °C, respectively. The decay of [(dppp)Pt(Me)(THF)]$^+$ (**3.27**) was more complex. In all cases, the addition of five equivalents of THF slowed the thermal degradation of the starting methyl derivatives, though the attenuation in decay rate was more pronounced for the cations (by approximately a factor of 2). The absence of first-order kinetics for cationic **3.27** can be attributed to the kinetically competitive degradation of [(dppp)Pt(Ph)(THF)]$^+$ (**4.7**) to the biphenyl complex **4.10**. An inhibitory build-up of THF occurs at such a rate that it complicates the kinetics of **3.27** by comparison to **3.11** and **3.26**.

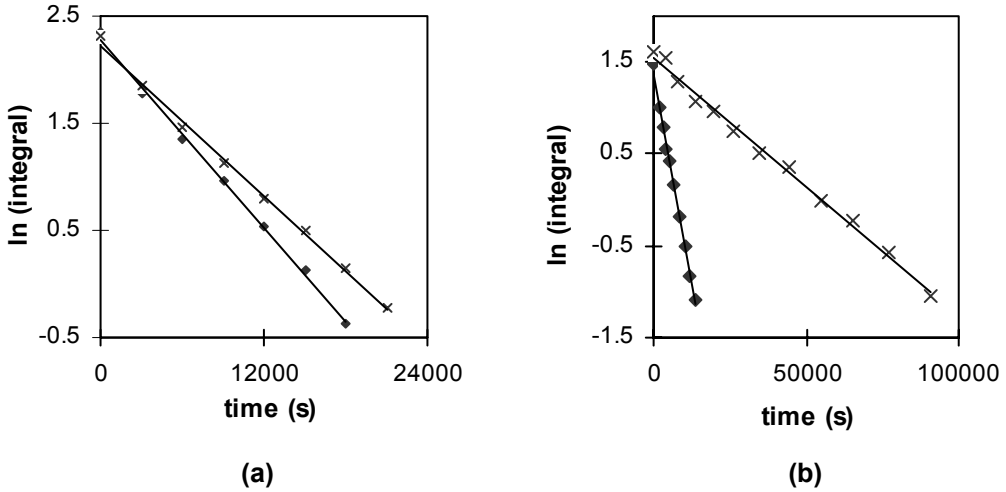

Figure 4.6. Representative plots of (a) $[Ph_2BP_2]Pt(Me)(THF)$ (**3.11**) in C_6H_6 (♦) and C_6D_6 (×) acquired at 45 ºC, and (b) $[(Ph_2SiP_2)Pt(Me)(THF)]^+$ (**3.26**) in C_6H_6 (♦) and C_6D_6 (×) acquired at 55 ºC.

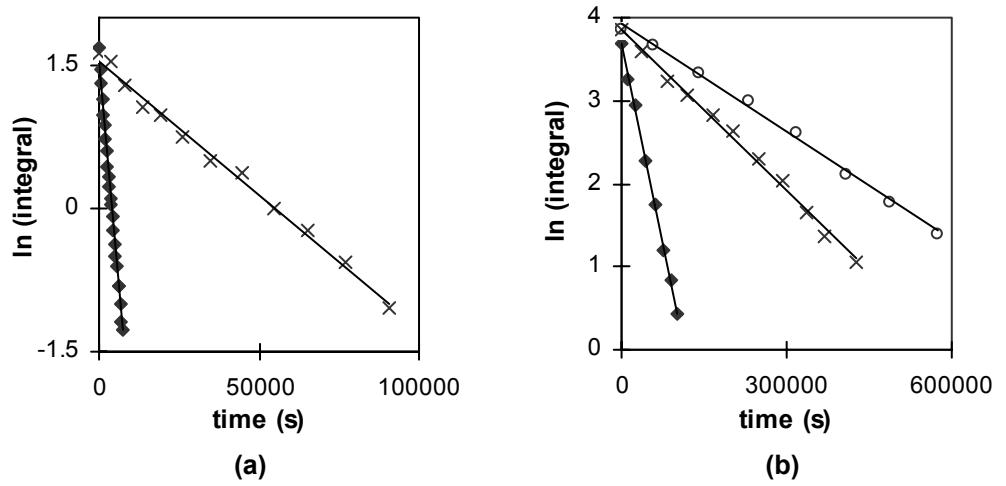

Figure 4.7. Representative plots of (a) $[Ph_2BP_2]Pt(Me)(THF)$ (**3.11**) (♦) and $[(Ph_2SiP_2)Pt(Me)(THF)]^+$ (**3.26**) (×) in C_6D_6 acquired at 55 ºC, and (b) **3.11** (♦), **3.26** (×), and $[(dppp)Pt(Me)(THF)]^+$ (**3.27**) (o) in C_6H_6 with 5 equivalents of THF acquired at 55 ºC.

For each system the benzene thermolysis of **3.11**, **3.26**, and **3.27** was carried out in both benzene and benzene-d_6. The measured $k(C_6H_6)/k(C_6D_6)$ ratio for $[Ph_2BP_2]Pt(Me)(THF)$ (**3.11**) at 45 ºC was 1.26. We were unable to make a comparable

measurement at 55 ºC due to the large errors in time introduced by using $^{31}P\{^{1}H\}$ NMR spectroscopy for this system. This value is strikingly different from that measured for $[(Ph_2SiP_2)Pt(Me)(THF)]^+$ (**3.26**) and that estimated for $[(dppp)Pt(Me)(THF)]^+$ (**3.27**) at 55 ºC. The measured $k(C_6H_6)/k(C_6D_6)$ ratio for **3.26** was 6.52 and that for **3.27** was similar, estimated to be approximately 6 by fitting the decay of **3.27** to a simple first-order model.

The effect on the rate of changing the ionic concentration of the solution was examined by the addition of one equivalent of $[^{n}Bu_4N][B(C_6F_5)_4]$. The addition of $[^{n}Bu_4N][B(C_6F_5)_4]$ to $[Ph_2BP_2]Pt(Me)(THF)$ (**3.11**) had no measurable effect on its observed rate of decay. However, the rate of decay of $[(Ph_2SiP_2)Pt(Me)(THF)]^+$ (**3.26**) was slowed somewhat by adding a stoichiometric equivalent of $[^{n}Bu_4N][B(C_6F_5)_4]$. It is worth noting that a second platinum compound was observed by $^{31}P\{^{1}H\}$ NMR spectroscopy upon addition of one equivalent of $[^{n}Bu_4N][B(C_6F_5)_4]$ to **3.26** that represented approximately 24% of the total integrated phosphorus resonances. The spectrum of this secondary species differs only slightly from the starting complex **3.26**, and it is tempting to assign this secondary species as the anion-coordinated ion-pair $[(Ph_2SiP_2)Pt(Me)]^+[(B(C_6F_5)_4)]^-$; however, we have not been able to rigorously isolate or thoroughly characterize this species.

4.2.5. Examination of alternative donor ligands for benzene C-H activation

In addition to THF as the coordinatively labile ligand in this study, we also considered alternative donor ligands. Several neutral $[Ph_2BP_2]Pt(Me)(L)$ complexes were prepared and cursorily examined for benzene C-H activation by thermolysis in benzene solution. Donor ligands were introduced to $[Ph_2BP_2]Pt(Me)(THF)$ (**3.11**) in THF solution to displace THF, providing $[Ph_2BP_2]Pt(Me)$(pyridine) (**4.11**), $[Ph_2BP_2]Pt(Me)$(pyridine-*N*-oxide) (**4.12**), $[Ph_2BP_2]Pt(Me)(SMe_2)$ (**4.13**), $[Ph_2BP_2]Pt(Me)(PMe_3)$ (**4.14**),

$[Ph_2BP_2]Pt(Me)(S{=}PMe_3)$ (**4.15**), and $[Ph_2BP_2]Pt(Me)\{P(C_6F_5)_3\}$ (**4.16**) (eq 4.16). In all cases, THF was displaced quantitatively as observed by $^{31}P\{^1H\}$ NMR spectroscopy. The zwitterionic complexes were isolated and subsequently thermolyzed in benzene solution. Of the complexes **4.11**-**4.16**, only **4.16** exhibited reactivity in benzene at 80 °C over one week.

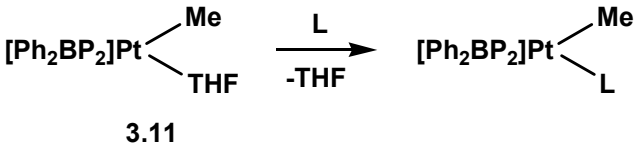

3.11

L = pyridine, 4.11
L = pyridine-*N*-oxide, 4.12
L = SMe_2, 4.13
L = PMe_3, 4.14
L = $S{=}PMe_3$, 4.15
L = $P(C_6F_5)_3$, 4.16

(4.16)

Based on the results of our donor ligand survey, we pursued the study of $[Ph_2BP_2]Pt(Me)\{P(C_6F_5)_3\}$ (**4.16**). We chose the phosphine $P(C_6F_5)_3$ as an appropriate L ligand candidate because of its relatively poor sigma donor ability and its unusually large Tolman cone angle (184º).[20] It also lacks potentially reactive aryl C-H bonds. We found that $P(C_6F_5)_3$ displaced THF from $[Ph_2BP_2]Pt(Me)(THF)$ (**3.11**) to provide the phosphine adduct complex **4.16** cleanly and in favorable crystalline yield (83%). A structural representation of complex **4.16**, along with a space filling representation, is shown in Figure 4.8. It is presumed from the solid-state structure of **4.16** that the $P(C_6F_5)_3$ coligand, in conjunction with the $[Ph_2BP_2]$ auxiliary, effectively blocks the platinum center with respect to associative approach of a fifth ligand.

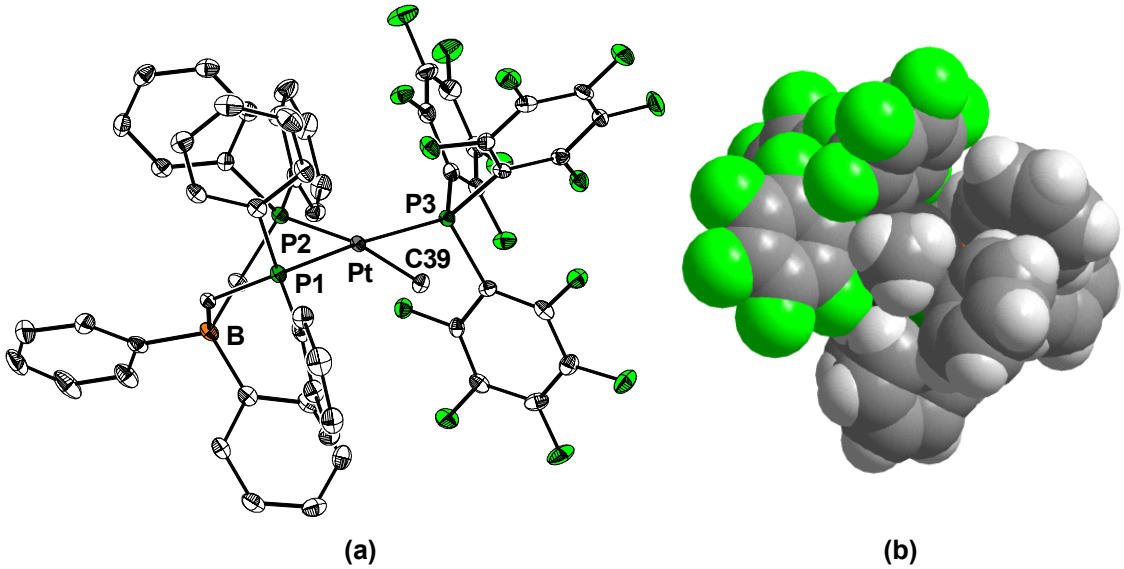

Figure 4.8. (a) Displacement ellipsoid representation (50%) of $[Ph_2BP_2]Pt(Me)\{P(C_6F_5)_3\}\cdot C_6H_6$ (**4.16·C$_6$H$_6$**). Hydrogen atoms and benzene solvent molecule are omitted for clarity. Selected interatomic distances (Å) and angles (º): Pt-C39, 2.120(3); Pt-P1, 2.3412(12); Pt-P2, 2.3361(10); Pt-P3, 2.2662(12); Pt-B, 3.845(4); C39-Pt-P1, 87.94(9); C39-Pt-P3, 81.40(9); P1-Pt-P2, 86.04(4); P2-Pt-P3, 104.89(4). (b) Space filling representation of **4.16**, looking down the platinum-methyl bond.

While the platinum center is buried beneath the protective organic aromatic rings, complex $[Ph_2BP_2]Pt(Me)\{P(C_6F_5)_3\}$ (**4.16**) nonetheless reacts in benzene to quantitatively form the phenyl complex $[Ph_2BP_2]Pt(Ph)\{P(C_6F_5)_3\}$ (**4.17**) with concomitant liberation of methane (eq 4.17). As might be expected, the benzene C-H activation process is much slower for **4.16** than for the corresponding THF adduct complex $[Ph_2BP_2]Pt(Me)(THF)$ (**3.11**). The half-life for **4.16** was approximately 230 minutes at 90 ºC. The product phenyl complex **4.17** was also appreciably more stable at this elevated temperature than that of its neutral THF counterpart $[Ph_2BP_2]Pt(Ph)(THF)$ (**4.5**), exhibiting no reactivity at 90 °C over 48 h. The addition of 5 equivalents of $P(C_6F_5)_3$ to a benzene solution of **4.16** significantly slowed its rate of decay.

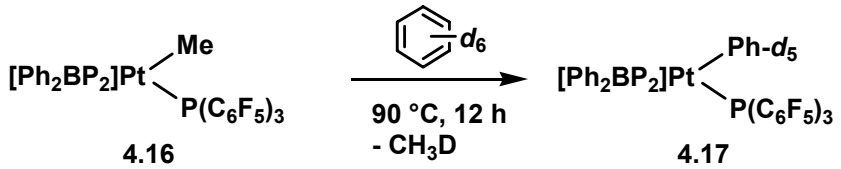

(4.17)

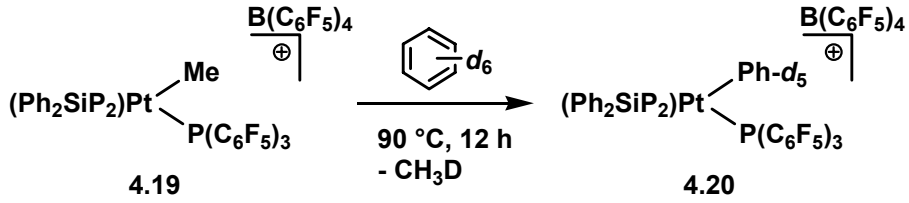

(4.18)

The analogous $P(C_6F_5)_3$-ligated cationic complex, $[(Ph_2SiP_2)Pt(Me)\{P(C_6F_5)_3\}][B(C_6F_5)_4]$ (**4.19**) was prepared similarly, and its thermolysis in benzene-d_6 was briefly examined (eq 4.18). Complex **4.19** underwent conversion to the cationic phenyl complex $[(Ph_2SiP_2)Pt(Ph)\{P(C_6F_5)_3\}][B(C_6F_5)_4]$ (**4.20**) at 90 ºC at a rate similar to the conversion of $[Ph_2BP_2]Pt(Me)\{P(C_6F_5)_3\}$ (**4.16**) to $[Ph_2BP_2]Pt(Ph)\{P(C_6F_5)_3\}$ (**4.17**). Complex **4.20** was, however, less stable than **4.17** under the thermolysis conditions and gradually afforded the dinuclear, biphenyl-bridged complex **4.9**. The collection of accurate rate data was precluded for **4.19** due to its poor solubility in benzene.

4.2.6. Isotopic incorporation into methane byproduct

The degree of deuterium incorporated into the methane byproduct was determined after thermolysis of complexes **3.11**, **3.26**, **3.27**, **4.16**, and **4.19** in benzene-d_6. The data are presented in Table 4.2. The nature of the methane byproduct released in the benzene-d_6 C-D bond activation reaction was examined by first executing each reaction in a sealed J. Young tube, and then inspecting the methane region of the ^{1}H NMR spectrum after completion of the reaction. The integrated ratio of the methane byproducts reported is taken as an average of three separate experiments. Only two

methane byproducts, CH_4 and CH_3D, were observed for each of these five systems, and in no case was either isotopomer produced exclusively. The relative ratio of the two byproducts favored CH_4 for neutral $[Ph_2BP_2]Pt(Me)(THF)$ (**3.11**): this result was markedly different from cationic $[(Ph_2SiP_2)Pt(Me)(THF)]^+$ (**3.26**) and $[(dppp)Pt(Me)(THF)]^+$ (**3.27**) and the bulky phosphine-ligated complexes $[Ph_2BP_2]Pt(Me)\{P(C_6F_5)_3\}$ (**4.16**) and $[(Ph_2SiP_2)Pt(Me)\{P(C_6F_5)_3\}]^+$ (**4.19**), all of which favored CH_3D. We also noted that the aryl region of the ^1H NMR spectrum of $[Ph_2BP_2]Pt(Me)(THF)$ (**3.11**) grew increasingly complex during the time course of its thermolysis (Figure 4.9), suggesting possible deuterium incorporation into the aryl positions of the $[Ph_2BP_2]$ ligand.

Table 4.2. Methane isotopomer ratios resulting from thermolysis of methyl complexes in benzene-d_6.

Compound	Temp	CH_4 : CH_3D
$[Ph_2BP_2]Pt(Me)(THF)$ (**3.11**)	55 ºC	3.0 : 1.0
$[Ph_2B(CH_2P(C_6D_5)_2)_2]Pt(Me)(THF)$ (**3.11-d_{20}**)	55 ºC	1.0 : 7.3
$[(Ph_2SiP_2)Pt(Me)(THF)]^+$ (**3.26**)	55 ºC	1.0 : 7.6
$[(dppp)Pt(Me)(THF)]^+$ (**3.27**)	55 ºC	1.0 : 5.8
$[Ph_2BP_2]Pt(Me)\{P(C_6F_5)_3\}$ (**4.16**)	90 ºC	1.0 : 5.9
$[(Ph_2SiP_2)Pt(Me)\{P(C_6F_5)_3\}]^+$ (**4.19**)	90 ºC	1.0 : 5.5

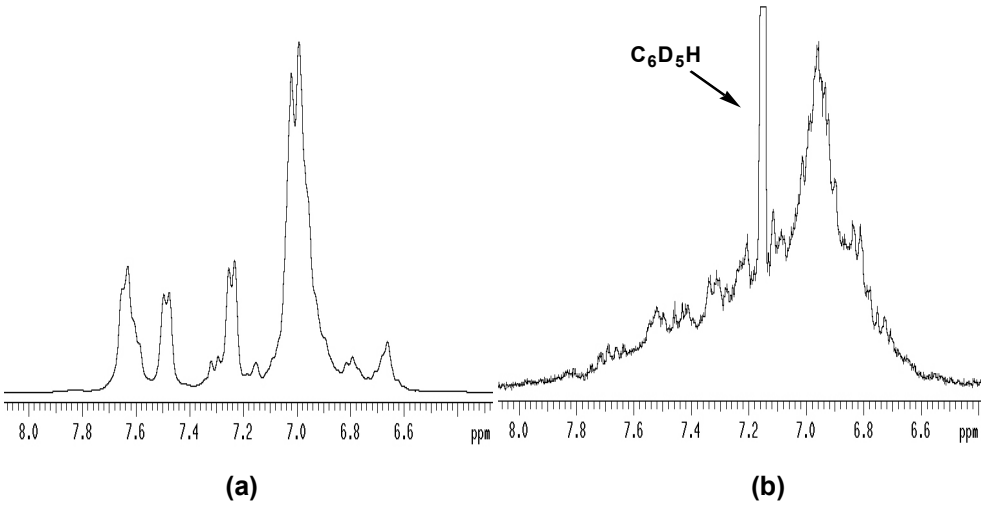

Figure 4.9. Representative ^{1}H NMR spectra of the aryl region of $[Ph_2BP_2]Pt(Me)(THF)$ (**3.11**) in benzene-d_6 (a) before thermolysis, and (b) after thermolytic conversion to predominantly complex $[Ph_2BP_2]Pt(Ph)(THF)$ (**4.5**). The complexity of spectrum (b) as compared to its corresponding $^{31}P\{^{1}H\}$ NMR spectrum suggests deuterium incorporation from benzene-d_6 into the $[Ph_2BP_2]$ ligand.

4.2.7. Spectral analysis of zwitterionic 3.11 in C_6D_6 – evidence for intermediate Pt(IV) species arising from reversible ligand metalation processes

The large quantity of CH_4 relative to CH_3D that was liberated when $[Ph_2BP_2]Pt(Me)(THF)$ (**3.11**) was incubated in benzene-d_6 suggested to us the possibility of reversible $[Ph_2BP_2]$ ligand metalation processes and prompted a closer examination of its $^{31}P\{^{1}H\}$ and ^{1}H NMR spectra at lower temperature. When a sample of **3.11** containing a few equivalents of excess THF was dissolved in benzene-d_6, its ^{1}H and $^{31}P\{^{1}H\}$ NMR spectra revealed complex **3.11** to be the only detectable solution species. However, when analytically pure **3.11**, obtained by careful drying under an argon or dinitrogen purge to remove residual THF, was dissolved in benzene-d_6 and examined at 25 °C by $^{31}P\{^{1}H\}$ NMR spectroscopy, additional resonances were immediately observed

that indicated the presence of species distinct from **3.11** (Figure 4.10). These species did not change significantly in concentration over time and appear to decay at rates similar to **3.11** under benzene thermolysis conditions. In contrast to neutral $[Ph_2BP_2]Pt(Me)(THF)$ (**3.11**), cationic complexes $[(Ph_2SiP_2)Pt(Me)(THF)]^+$ (**3.26**) and $[(dppp)Pt(Me)(THF)]^+$ (**3.27**) provided unremarkable NMR spectra at 25 ºC in benzene and in benzene-d_6, indicative of the presence of a single solution species (Figure 4.11). Selected regions of the $^{31}P\{^1H\}$ and $^1H\{^{31}P\}$ NMR spectra of **3.11** in benzene-d_6 at 25 °C are shown in Figure 4.10 to aid in their interpretation.

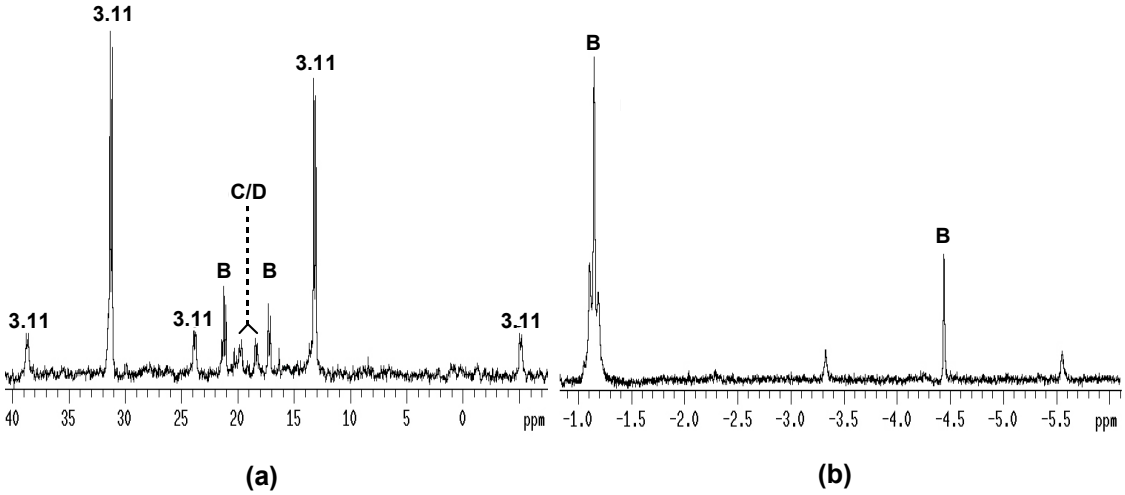

Figure 4.10. Representative NMR spectra of complex $[Ph_2BP_2]Pt(Me)(THF)$ (**3.11**) at 25 ºC in benzene-d_6 showing (a) the $^{31}P\{^1H\}$ NMR spectrum containing the expected resonances for **3.11** and additional resonances corresponding to species **B**, **C**, and **D**, and (b) the $^1H\{^{31}P\}$ NMR spectrum of methyl and hydride resonances assigned to species **B**.

Examination of the $^{31}P\{^1H\}$ NMR spectrum of $[Ph_2BP_2]Pt(Me)(THF)$ (**3.11**) dissolved in C_6D_6 at 25 ºC displayed three sets, and possibly a fourth set, of resonances, signifying multiple species in solution (Figure 4.10a). The major set of resonances (labeled **3.11**; approximately 80%) appears as two doublets at 34.1 and 16.1 ppm ($^2J_{P\text{-}P}$ =

22 Hz), respectively, and corresponds to complex **3.11**. Another set of signals arising as two doublets centered at 23.0 and 19.3 ppm ($^2J_{P\text{-}P}$ = 20 Hz), respectively, labeled **B**, represents approximately 10% of the total integrated intensity. There is a third, and perhaps fourth, set of resonances in the $^{31}P\{^1H\}$ NMR spectrum (labeled **C** and **D**) centered at 21.7 and 20.4 ppm that may be assigned as doublets with P-P coupling evident ($^2J_{P\text{-}P} \approx 20$ Hz). These signals represent only about 5-7% of the total integrated intensity and correspond to possibly two other species.

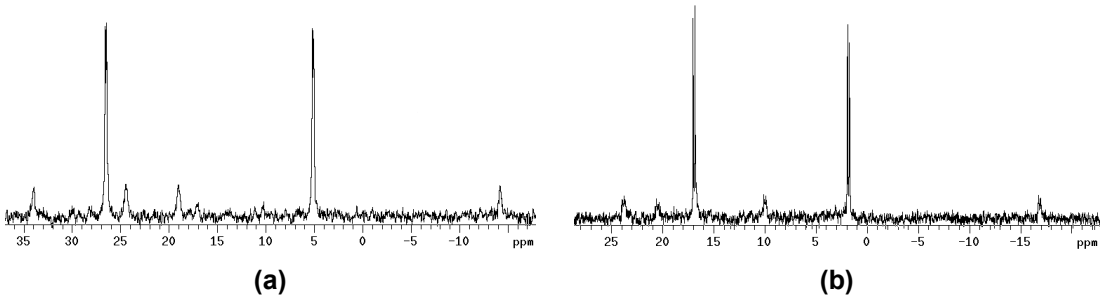

Figure 4.11. Room temperature $^{31}P\{^1H\}$ NMR spectra in benzene-d_6 of (a) $[(Ph_2SiP_2)Pt(Me)(THF)][B(C_6F_5)_4]$ (**3.26**) and (b) [(dppp)Pt(Me)(THF)] $[B(C_6F_5)_4]$ (**3.27**).

To further examine the additional species in solution, the $^1H\{^{31}P\}$ NMR spectrum of $[Ph_2BP_2]Pt(Me)(THF)$ (**3.11**) in C_6D_6 was also examined at 25 ºC. The $^1H\{^{31}P\}$ NMR spectrum of the same sample reveals a well-defined hydride signal at -4.4 ppm, ($^1J_{Pt\text{-}H}$ = 667 Hz), and a distinct methyl resonance at -1.2 ppm with ^{195}Pt satellites ($^2J_{Pt\text{-}H}$ = 24 Hz) that is well separated from the more intense methyl resonance of **3.11** (Figure 4.10b). These methyl and hydride resonances appear to correlate to the $^{31}P\{^1H\}$ NMR resonances assigned to **B**, in that they all appear to decay at similar rates as $[Ph_2BP_2]Pt(Me)(THF)$ (**3.11**) is slowly converted to $[Ph_2BP_2]Pt(Ph)(THF)$ (**4.5**) at 25 °C. Also, the methyl resonance assigned to **B** integrates as three times the intensity of the hydride resonance.

Therefore, we assign a hydride, a methyl, and a [Ph_2BP_2] ligand to a single platinum center in **B**, which we think is most consistent with a [Ph_2BP_2]-metalated platinum(IV) complex. Because the hydride signal we assign to **B** is present even when the deuterated system [$Ph_2B(CH_2P(C_6D_5)_2)_2$]Pt(Me)(THF) (**3.11-*d*$_{20}$**) is examined (*vide infra*), we suggest that **B** is a platinum(IV) product derived from metalation at the diphenylborate unit of the [Ph_2BP_2] ligand, rather than an arylphosphine position. Moreover, the chemical shift and coupling data for the hydride and methyl ligands of **B** are consistent with their being *trans* to a phosphine donor of the [Ph_2BP_2] ligand.[21] These NMR data are consistent with two possible structures (Figure 4.12) for the intermediate referred to as **B** that we cannot distinguish. Both five- and six-coordinate platinum(IV) species have literature precedent, though six-coordinate structures are more common.[22]

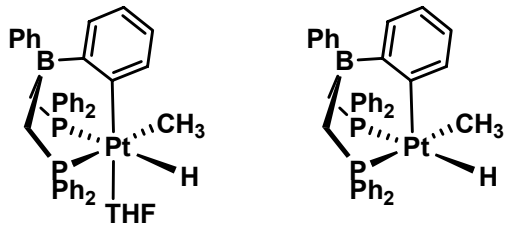

Figure 4.12. Possible structures for the ortho-metalated platinum(IV) methyl hydride intermediate **B**. Both five- and six-coordinate geometries for **B** can be envisioned.

At least one and possibly two other methyl resonances distinct from those for [Ph_2BP_2]Pt(Me)(THF) (**3.11**) and **B** could also be distinguished in the $^1H\{^{31}P\}$ NMR spectrum. More data is provided below to verify the presence of four spectroscopically detectable methyl-containing species when pure **3.11** is dissolved in benzene-d_6 at 25 °C. The only well-resolved hydride signal that could be assigned with confidence at 25 °C, however, was that arising from **B**.

4.2.8. Preparation of the ^{13}C-labeled complex [Ph_2BP_2]Pt($^{13}CH_3$)(THF) (**3.11**-$^{13}CH_3$) and its characterization by NMR spectroscopy in benzene-d_6 at 25 °C

To more definitively determine the number of methyl-containing species in solution, we incorporated a ^{13}C-labeled methyl group into complex [Ph_2BP_2]Pt(Me)(THF) (**3.11**). Preparation of [Ph_2BP_2]Pt($^{13}CH_3$)(THF) (**3.11**-^{13}**CH$_3$**) proceeded by the same method as for **3.11**, using (COD)Pt($^{13}CH_3)_2$[23] as the starting platinum material. Dissolving [Ph_2BP_2]Pt($^{13}CH_3$)(THF) (**3.11**-^{13}**CH$_3$**) in C_6D_6 and examining its NMR spectra at 25 ºC provided additional information about the species in solution. Definitely three and more likely four distinct sets of platinum-bound methyl resonances could be discerned in the ^{1}H{^{31}P} NMR spectrum of **3.11**-^{13}**CH$_3$**. The methyl resonances of **3.11**-^{13}**CH$_3$** that correlate to those assigned for unlabeled [Ph_2BP_2]Pt(Me)(THF) (**3.11**) showed the expected $^1J_{C\text{-}H}$ coupling arising from the labeled carbon in **3.11**-^{13}**CH$_3$**, and the signature ^{195}Pt satellites were discernable. The hydride signal at -4.4 ppm remained unchanged by comparison to the unlabeled derivative **3.11**. We conclude that *cis* two-bond coupling between the methyl and hydride ligands of species **B** is therefore not resolvable.

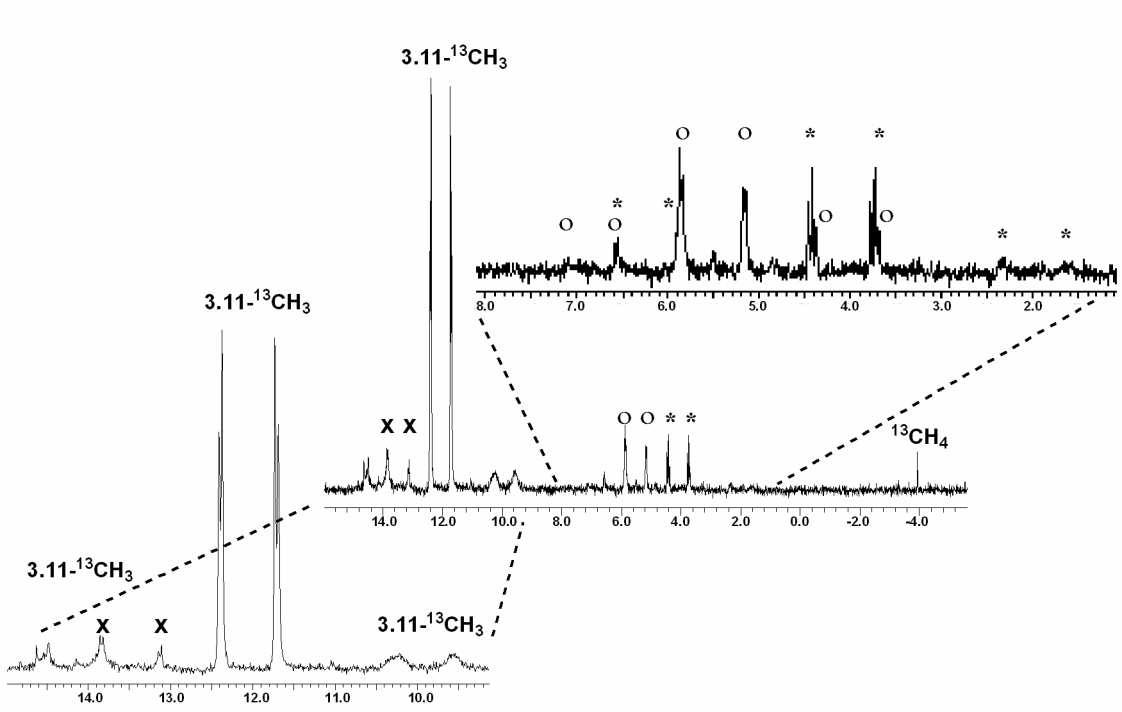

Figure 4.13. $^{13}C\{^1H\}$ NMR spectrum of $[Ph_2BP_2]Pt(^{13}CH_3)(THF)$ (**3.11-^{13}CH$_3$**) when dissolved in benzene-d_6 at 25 °C. The spectrum shows four distinct sets of platinum methyl resonances, the major set corresponding to complex **3.11-^{13}CH$_3$** itself, and the other species are labeled ×, o, and ∗.

The presence of four discrete methyl resonances in the benzene-d_6 $^{13}C\{^1H\}$ NMR spectrum of $[Ph_2BP_2]Pt(^{13}CH_3)(THF)$ (**3.11-^{13}CH$_3$**), presented in Figure 4.13, corroborates our assignment of four distinct species in the $^{31}P\{^1H\}$ NMR spectrum of $[Ph_2BP_2]Pt(Me)(THF)$ (**3.11**), although we cannot definitively correlate the observed signals. The $^2J_{P\text{-}C}$ coupling can be discerned in each resonance and, in three cases, the ^{195}Pt satellites are observed. One doublet of doublets at 12.0 ppm (labeled **3.11-^{13}CH$_3$**, $^1J_{Pt\text{-}C}$ = 543 Hz, $^2J_{P\text{-}C}$ = 4.4, 85 Hz) is consistent with the previously observed methyl for unlabeled $[Ph_2BP_2]Pt(Me)(THF)$ (**3.11**). Three additional doublets of doublets are also present, and are labeled as ×, o, and ∗ in Figure 4.13. The signal for species × (13.5 ppm, $^2J_{P\text{-}C}$ = 5, 90 Hz) is partially obscured by the platinum satellites of the methyl group of

3.11-^{13}CH$_3$, and its low intensity prevents the detection of platinum coupling. The signals assigned as o and * are separated from **3.11-^{13}CH$_3$** and ×, and each displays coupling to one platinum and two phosphorus atoms, arising at 5.5 ppm ($^1J_{Pt-C}$ = 367 Hz, $^2J_{P-C}$ = 5, 88 Hz) and 4.1 ppm ($^1J_{Pt-C}$ = 525 Hz, $^2J_{P-C}$ = 6, 86 Hz), respectively. Each of these signals displays coupling to ^{31}P that is consistent with one *cis* and one *trans* relationship.

The region between 150 and 400 ppm of the ^{13}C{^{1}H} NMR spectrum was also carefully inspected for the presence of any "methylene-hydride" type species, such as [Ph$_2$BP$_2$]Pt=CH$_2$(H), that might arise from α-hydride migration processes exhibited by [Ph$_2$BP$_2$]Pt(^{13}CH$_3$)(THF) (**3.11-^{13}CH$_3$**). No evidence for any such species was obtained. Formation of a carbene-hydride species from a THF activation process with concomitant expulsion of methane would also have been plausible given that such a process was observed for the cationic system [(TMEDA)Pt(Me)(L)]$^+$ (L = OEt$_2$, THF) reported by Holtcamp, Labinger and Bercaw. Further confirmation that carbene hydrides are not formed from activation of the THF ligand in the case of [Ph$_2$BP$_2$]Pt(Me)(THF) (**3.11**) is that the signal due to ^{13}CH$_4$ in Figure 4.13 is very weak. This signal most likely results from very modest benzene or ligand activation at 25 °C during the time course of the data collection (hours). We conclude that the species **B**, **C**, and **D** that were observed in the ^{31}P{^{1}H} NMR of **3.11** each contain a methyl group and are therefore formed prior to reductive elimination of methane.

4.2.9. Spectroscopic characterization, and benzene reaction chemistry of the *d*$_{20}$-labeled complex [Ph$_2$B(CH$_2$P(C$_6$D$_5$)$_2$)$_2$]Pt(Me)(THF) (3.11-*d*$_{20}$)

The complex [Ph$_2$B(CH$_2$P(C$_6$D$_5$)$_2$)$_2$]Pt(Me)(THF) (**3.11-*d*$_{20}$**) was studied by ^{1}H and ^{2}H NMR spectroscopies. Most important was the use of these spectra to aid the

assignment of **B**. The hydride signal at -4.4 ppm that appears when $[Ph_2BP_2]Pt(Me)(THF)$ (**3.11**) is dissolved in benzene-d_6 is still present in the ^1H NMR spectrum of **3.11-*d*$_{20}$**: its intensity is not appreciably diminished, as would be expected if the hydride were derived from the *d*-labeled phenylphosphines. The ^2H NMR spectrum of **3.11-*d*$_{20}$** was inspected, and no platinum deuteride was detected. As mentioned above, we interpret these data by formulating **B** as a platinum(IV) methyl hydride metalated at the diphenylborate position.

Two other important results were revealed from examination of the rate of benzene C-H bond activation exhibited by $[Ph_2B(CH_2P(C_6D_5)_2)_2]Pt(Me)(THF)$ (**3.11-*d*$_{20}$**). The rate of decay of **3.11-*d*$_{20}$** was observed in benzene and benzene-d_6 at 55 ºC, and the half-lives were approximately 54 min and 95 min, respectively. This provided an isotope effect of $k(C_6H_6)/k(C_6D_6) \approx 1.8$. Also, the rate of decay of **3.11-*d*$_{20}$** was about three times slower than that of unlabeled $[Ph_2BP_2]Pt(Me)(THF)$ (**3.11**) in benzene-d_6 at 55 °C, providing a $k_{\mathbf{3.11}}/k_{\mathbf{3.11}\text{-}d_{20}}$ of approximately 3 between the two systems. Additionally, the methane byproduct released during the benzene-d_6 thermolysis of **3.11-*d*$_{20}$** showed predominantly CH_3D (1.0 *CH_4*: 7.3 *CH_3D*) rather than CH_4, as was the case for **3.11** (Table 4.2). The implication of these labeling results to the overall solution chemistry of **3.11** will be more thoroughly discussed in the next section. We note for now the likelihood that reversible metalation at a phenylphosphine arm of **3.11** is likely operative and is a contributing factor to the rate of its intermolecular benzene C-H activation chemistry.

Considering the NMR data for $[Ph_2BP_2]Pt(Me)(THF)$ (**3.11**), $[Ph_2BP_2]Pt(^{13}CH_3)(THF)$ (**3.11-^{13}CH$_3$**), and $[Ph_2B(CH_2P(C_6D_5)_2)_2]Pt(Me)(THF)$ (**3.11-**

***d*$_{20}$**) as a whole, it is possible to assign with confidence complex **3.11** and intermediate **B**. Species **C** and **D** may represent isomers of a ligand-metalated species, in which we do not observe the hydride signals, but we speculate that they more likely represent stable Pt(II) species where THF is no longer coordinated in the fourth position. Other alternative ligands that would occupy that site include a benzene adduct, an isomer in which the [Ph_2BP_2] ligand is bound η^3, or perhaps a three-coordinate platinum center, the latter possibility seeming less likely. Given the recent characterization of an η^2-benzene adduct of platinum(II)[10b] and that benzene is the solvent, we propose that one of species **C** or **D** is most likely [Ph_2BP_2]Pt(Me)(η^2-benzene).

4.3. Mechanistic discussion

4.3.1. Comparative aspects of benzene C-H activation chemistry exhibited by 3.11 and 3.26

Complexes [Ph_2BP_2]Pt(Me)(THF) (**3.11**), [(Ph_2SiP_2)Pt(Me)(THF)]$^+$ (**3.26**), and [(dppp)Pt(Me)(THF)]$^+$ (**3.27**) each react in benzene to generate the phenyl derivatives [Ph_2BP_2]Pt(Ph)(THF) (**4.5**), [(Ph_2SiP_2)Pt(Ph)(THF)]$^+$ (**4.6**), and [(dppp)Pt(Ph)(THF)]$^+$ (**4.7**), respectively. Our primary aim in this section is to assemble the many pieces of data presented into a reasonable model that describes the benzene solution chemistry of neutral **3.11** in comparison to its cationic analogues **3.26** and **3.27**. Within this context, we will try to describe the mechanisms by which benzene enters the coordination sphere of the respective platinum centers, the factors that dictate the rate at which it undergoes C-H activation, and the role of the ancillary phosphine ligand in each case. Because the solution chemistries of cationic **3.26** and **3.27** appear to be similar, we confine our comparative discussion to systems [Ph_2BP_2]Pt(Me)(THF) (**3.11**) and

$[(Ph_2SiP_2)Pt(Me)(THF)]^+$ (**3.26**) and note by analogy that our conclusions between these two systems map to similar conclusions between **3.11** and $[(dppp)Pt(Me)(THF)]^+$ (**3.27**).

The measured rates of first-order decay exhibited by $[Ph_2BP_2]Pt(Me)(THF)$ (**3.11**) and $[(Ph_2SiP_2)Pt(Me)(THF)]^+$ (**3.26**) in both benzene and benzene-d_6 provide important data. As can been seen in Table 4.1, complex **3.11** reacts more quickly towards intermolecular benzene C-H activation than **3.26**. At the outset of our study, much attention was being drawn to increasingly electrophilic platinum systems,[5-12] the rationale being that more electrophilic systems would undergo C-H activation more rapidly. This study, in addition to recent studies by Bercaw and Bergman, establishes that a variety of factors dominate the overall rate of intermolecular C-H activation and that electronic factors can play an indirect, often non-intuitive, role.

Due in part to the pronounced kinetic deuterium isotope effect measured for $[(Ph_2SiP_2)Pt(Me)(THF)]^+$ (**3.26**), $k(C_6H_6)/k(C_6D_6)$ = 6.52 at 55 ºC, compared to the modest effect measured for $[Ph_2BP_2]Pt(Me)(THF)$ (**3.11**), $k(C_6H_6)/k(C_6D_6)$ = 1.26 at 45 ºC, the rate of C-D activation in benzene-d_6 is approximately fourteen times faster for **3.11** than it is for **3.26** ($t_{1/2}$ at 55 °C = 31 and 430 min, respectively). If we assume that the isotope effect remains relatively constant over temperature, we can extrapolate that the difference in rates in C_6H_6 at 55 °C to be small, however, with $[Ph_2BP_2]Pt(Me)(THF)$ (**3.11**) being about a factor of two faster. *The measured differences in absolute rate reflect different operative mechanisms* and therefore do not clearly provide information concerning how the relative electrophilicities of each system correlate to the rate of the elementary C-H bond-breaking step they each exhibit.

Each case showed a slowing of the rate of C-H activation in the presence of additional equivalents of THF. It seems reasonable to assume for cationic $[(Ph_2SiP_2)Pt(Me)(THF)]^+$ (**3.26**) that THF is competing with benzene to bind to the metal center, in accord with the THF self-exchange data acquired in benzene-d_6. Given that k_{ex} for neutral $[Ph_2BP_2]Pt(Me)(THF)$ (**3.11**) shows no [THF] dependence for THF self-exchange, we interpret the [THF] dependence of the decay rate of **3.11** in benzene to imply that the addition of THF affects an equilibrium process preceding C-H activation which is not ligand self-exchange.

4.3.2. Evidence for reversible ligand metalation processes operative in the chemistry of neutral 3.11

The solution NMR data obtained for unlabeled $[Ph_2BP_2]Pt(Me)(THF)$ (**3.11**) and its ^{13}C-CH_3 and d_{20}-$[Ph_2BP_2]$-labeled derivatives $[Ph_2BP_2]Pt(^{13}CH_3)(THF)$ (**3.11-^{13}CH$_3$**) and $[Ph_2B(CH_2P(C_6D_5)_2)_2]Pt(Me)(THF)$ (**3.11-*d*$_{20}$**) allow us to suggest that reversible $[Ph_2BP_2]$ ligand metalation processes dominate the chemistry of neutral **3.11**. In comparison, the solution data obtained for $[(Ph_2SiP_2)Pt(Me)(THF)]^+$ (**3.26**) and $[(dppp)Pt(Me)(THF)]^+$ (**3.27**) provide no direct evidence for related processes. Inspection of the $^{31}P\{^1H\}$ NMR spectrum of analytically pure **3.26** and **3.27** at 25 °C showed only a single species, consistent with this assertion. While the observation of small amounts of CH_4 upon thermolysis of $[(Ph_2SiP_2)Pt(Me)(THF)]^+$ (**3.26**) and $[(dppp)Pt(Me)(THF)]^+$ (**3.27**) in benzene-d_6 suggests the likelihood that ligand activation processes may be operative to some extent, they are much less prevalent than for **3.11**. For neutral $[Ph_2BP_2]Pt(Me)(THF)$ (**3.11**), $[Ph_2BP_2]$ metalation processes involve both the arylphosphine positions and the diphenylborate unit. The NMR data provide strong evidence for a spectroscopically observable platinum(IV) methyl hydride (intermediate

B), a species that would result from metalation of the diphenylborate unit. Species such as **B** are typically not observable due to facile reductive elimination to regenerate platinum(II). The chelate structure postulated for **B** (Figure 4.12) is expected to be stable given the excellent chelate properties of the tris(phosphino)borate ligand $[PhB(CH_2PPh_2)_3]$,[24] a tripodal ligand whose chelate ring sizes compare well with those shown in **B**. If our assignment of **B** is correct, neutral $[Ph_2BP_2]Pt(Me)(THF)$ (**3.11**) represents the first system in which a *reversibly formed* platinum(IV) intermediate is observable within a platinum(II) system that also mediates a well-defined, intermolecular C-H bond activation process. Given the similarity between a $[Ph_2BP_2]$ phenyl ring substrate and benzene itself, it is quite reasonable to suggest that the intermolecular benzene activation process also proceeds via a platinum(II/IV) couple, as has been asserted for related platinum(II) systems that display intermolecular C-H activation chemistry.[5-12]

It appears to be possible to inhibit ligand metalation processes prevalent in $[Ph_2BP_2]Pt(Me)(THF)$ (**3.11**) by turning to an L-type ligand that is more sterically encumbered. Such a comparison is provided by the solution chemistry of $[Ph_2BP_2]Pt(Me)\{P(C_6F_5)_3\}$ (**4.16**). While **4.16** exhibits a similar benzene C-H activation reaction, thermolysis of **4.16** in benzene-d_6 gives rise to a very different ratio in the released methane isotopomers by comparison to **3.11**. The observed ratio for $[Ph_2BP_2]Pt(Me)\{P(C_6F_5)_3\}$ (**4.16**) was very similar to that observed for its cationic analogue $[[Ph_2SiP_2]Pt(Me)\{P(C_6F_5)_3\}]^+$ (**4.19**). To explain these data, we suggest that the steric bulk of **4.16** prohibits anchimeric η^3-binding of its $[Ph_2BP_2]$ ligand, thereby attenuating $[Ph_2BP_2]$ ligand metalation processes that favor the release of CH_4 over

CH_3D. Worth noting is that the $^{31}P\{^1H\}$ and ^1H NMR spectra of **4.16** indicate a single solution species prior to and during thermolysis, similar to the case for $[(Ph_2SiP_2)Pt(Me)(THF)]^+$ (**3.26**) and $[(dppp)Pt(Me)(THF)]^+$ (**3.27**).

4.3.3. Overall mechanistic summary

The benzene solution chemistry we have observed for neutral $[Ph_2BP_2]Pt(Me)(THF)$ (**3.11**) is generally comparable to that observed for its isostructural but cationic relatives $[(Ph_2SiP_2)Pt(Me)(THF)]^+$ (**3.26**) and $[(dppp)Pt(Me)(THF)]^+$ (**3.27**). Each system mediates an intermolecular benzene C-H bond activation process under a similar set of reaction conditions. The zwitterionic description of neutral $[Ph_2BP_2]Pt(Me)(THF)$ (**3.11**) seems to predict its overall reactivity in comparison to structurally related cationic complexes. However, important mechanistic differences exist that can be attributed to the role that the bis(phosphine) ligand auxiliary plays in each respective system. These mechanistic distinctions most likely reflect electronic rather than steric differences. The most relevant mechanistic points are summarized in Table 4.3 and underscore the observation that $[Ph_2BP_2]Pt(Me)(THF)$ (**3.11**) appears to undergo ligand metalation chemistry.

Table 4.3. Summary of key mechanistic observables for the reaction of **3.11** and **3.26** in benzene.

$[Ph_2BP_2]Pt(Me)(THF)$ **3.11** $\xrightarrow[-\ CH_4 \text{ or } CH_3D]{PhH \text{ or } PhD}$ $[Ph_2BP_2]Pt(Ph)(THF)$ **4.5**	$[(Ph_2SiP_2)Pt(Me)(THF)]^{\oplus}$ **3.26** $\xrightarrow[-\ CH_4 \text{ or } CH_3D]{PhH \text{ or } PhD}$ $[(Ph_2SiP_2)Pt(Ph)(THF)]^{\oplus}$ **4.6**
• Rate of C-H activation at 45 °C: $k = 1.42(5) \times 10^{-4}\ s^{-1}$ • Rate of C-D activation at 45 °C: $k = 1.13(3) \times 10^{-4}\ s^{-1}$ • $k(C_6H_6)/k(C_6D_6)$ at 45 °C for **3.11** = 1.26 • $k(C_6H_6)/k(C_6D_6)$ at 45 °C for **3.11-d_{20}** = 1.8 • $k_{3.11}/k_{3.11\text{-}d_{20}}$ in C_6D_6 at 55 °C is ≈ 3.1 • $k_{3.11}/k_{3.11\text{-}d_{20}}$ in C_6H_6 at 55 °C is ≈ 2	• Rate of C-H activation at 55 °C: $k = 1.80(6) \times 10^{-4}\ s^{-1}$ • Rate of C-D activation at 55 °C: $k = 2.76(7) \times 10^{-5}\ s^{-1}$ • $k(C_6H_6)/k(C_6D_6)$ at 55 °C for **3.26** = 6.52 • $k_{3.11}/k_{3.26}$ in C_6D_6 at 55 °C is ≈ 14 • $k_{3.11}/k_{3.26}$ in C_6H_6 at 55 °C is ≈ 2.5
• Mechanism of THF self-exchange is ligand-assisted (or dissociative). • Activation parameters: $\Delta S^{\ddagger}_{298K} = -0.1 \pm 5.4$ e.u. and $\Delta H^{\ddagger} = 16.0 \pm 1.6$ kcal/mol	• Mechanism of THF self-exchange is associative. • Activation parameters: $\Delta S^{\ddagger}_{298K} = -30.2 \pm 5.2$ e.u. and $\Delta H^{\ddagger} = 1.9 \pm 0.5$ kcal/mol
• *CH_4 : CH_3D* ratio in methane byproduct after thermolysis of **3.11** in C_6D_6: *3.0 : 1.0.* • *CH_4 : CH_3D* ratio in methane byproduct after thermolysis of **3.11-d_{20}** in C_6D_6: *1.0: 7.3*.	• *CH_4 : CH_3D* ratio in methane byproduct after thermolysis of **3.26** in C_6D_6: *1.0 : 7.6*
• Significant deuterium incorporation into the $[Ph_2BP_2]$ ligand after thermolysis in benzene-d_6.	• Negligible deuterium incorporation into the (Ph_2SiP_2) ligand after thermolysis in benzene-d_6.
• $[Ph_2BP_2]$ metalation in benzene solution is kinetically very competitive with benzene C-H activation processes. • Several spectroscopically observable intermediates.	• (Ph_2SiP_2) metalation in benzene solution is kinetically non-competitive with benzene C-H activation processes. • No spectroscopically observable intermediates.

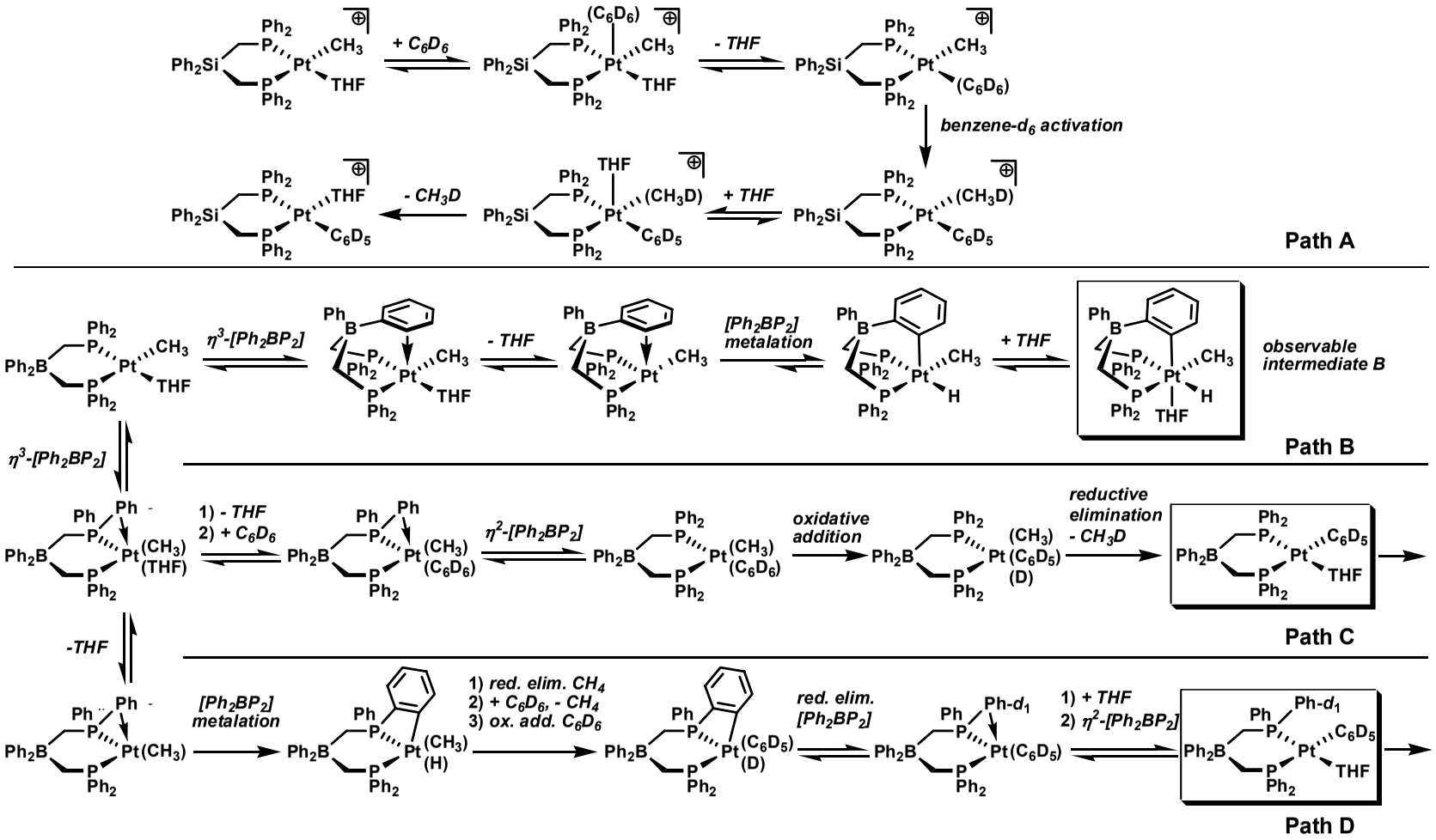

Figure 4.14. Postulated mechanisms for the predominant pathways leading to intermolecular benzene C-H activation chemistry for cationic $[(Ph_2SiP_2)Pt(Me)(THF)]^+$ (**3.26**) (upper mechanism, **Path A**) and zwitterionic $[Ph_2BP_2]Pt(Me)(THF)$ (**3.11**) (lower mechanism, **Path B**, **Path C**, and **Path D**).

For the cationic system $[(Ph_2SiP_2)Pt(Me)(THF)]^+$ (**3.26**) (and by analogy $[(dppp)Pt(Me)(THF)]^+$, **3.27**), the neutral bis(phosphine) chelate appears to be relatively innocent with respect to the C-H activation and THF exchange chemistry studied. From the THF self-exchange data for $[(Ph_2SiP_2)Pt(Me)(THF)]^+$ (**3.26**), we infer that ligand substitution proceeds in a bimolecular, associative fashion. We infer that this is also true for benzene displacement of THF in benzene solution, a process we could not measure directly but can reasonably deduce by comparison to the THF self-exchange data. The C-H activation processes that occur in benzene solution for **3.26** appear also to be predominantly intermolecular in nature. Although we cannot rule out the possibility of reversible ligand metalation processes operative in the benzene solution chemistry of **3.26** as a small amount of CH_4 is observed as a byproduct upon thermolysis of **3.26** in benzene-d_6, we suggest that any intramolecular activation processes are sufficiently dominated by intermolecular processes that it is a justifiable simplification to mechanistically focus on the latter type. In Figure 4.14, we outline the simplest plausible mechanism (**Path A**) by which cationic **3.26** undergoes intermolecular benzene activation. The outlined mechanism is consistent with our data and is generally similar to that proposed for other $L_2Pt(Me)^+$ systems that have been thoroughly described elsewhere.[5-12] *Key points to note in **Path A** are that benzene coordination to the cationic platinum center is likely an associative process, and the benzene activation step is likely to be rate-determining as suggested by the large primary kinetic isotope effect that was observed for* **3.26** *($k(C_6H_6)/k(C_6D_6) = 6.52$).* While we might favor a benzene C-H activation step for the cationic system that occurs by oxidative addition from platinum(II)

to give a platinum(IV) phenyl hydride, our data is unbiased and neither supports nor refutes this hypothesis.

The neutral system $[Ph_2BP_2]Pt(Me)(THF)$ (**3.11**) differs from $[(Ph_2SiP_2)Pt(Me)(THF)]^+$ (**3.26**) in that the bis(phosphine) ligand **2.25** appears to be intimately involved in both ligand exchange and C-H activation processes operative in benzene solution. The zero-order dependence in THF for THF self-exchange reflects the ability of the $[Ph_2BP_2]$ ligand to assist in ligand exchange by an η^3-binding mode, an intramolecular process akin to a solvent-assisted ligand substitution process. While THF loss might also be dissociative based upon our exchange data, the prevailing ligand metalation chemistry of $[Ph_2BP_2]Pt(Me)(THF)$ (**3.11**) persuades us to discount this latter possibility. This propensity for the $[Ph_2BP_2]$ ligand to achieve an η^3-binding mode dramatically impacts the nature of the C-H activation processes that are observed in benzene solution.

In Figure 4.14, we outline three mechanistic pathways to account for the solution chemistry of $[Ph_2BP_2]Pt(Me)(THF)$ (**3.11**). These are labeled **Path B**, **Path C**, and **Path D**, respectively. Association of an aryl ring from the diphenylborate unit of **3.11** leads down **Path B** to a metalation process that generates a platinum(IV) methyl hydride complex (product **B**), an intermediate that can be spectroscopically detected. We do not think product **B** precedes an intermolecular benzene C-H activation step. Rather, we think that metalation at the diphenylborate unit is reversible and that product **B** is ultimately funneled along **Path C** and **Path D**. Common to **Path C** and **Path D** is an η^3-binding mode for the $[Ph_2BP_2]$ auxiliary that involves the arylphosphine donor rather than the diphenylborate unit. **Path C** proceeds along a simpler scenario that invokes a

[Ph_2BP_2]-assisted benzene-d_6 substitution for THF, followed by oxidative addition of benzene-d_6 and reductive elimination of the expected methane byproduct CH_3D. *The key distinction between* ***Path C*** *and* ***Path A*** *is the mechanism by which benzene enters the platinum coordination sphere. On the basis of our isotopic labeling, activation, and incorporation studies, we propose that the rate-determining step along* ***Path C*** *is the ligand C-H activation step, and that the negligible primary kinetic isotope effect that was measured for [Ph_2BP_2]Pt(Me)(THF) (**3.11**) ($k(C_6H_6)/k(C_6D_6) = 1.26$) is due to the kinetic dominance of the fourth path,* ***Path D***. In this last pathway, arylphosphine ligand metalation processes occur that produce platinum(IV) methyl hydride-species distinct from product **B** (shown in **Path B**). Following ligand metalation, benzene-d_6 enters the platinum coordination sphere at one of several indistinguishable stages, each of which involves the reductive elimination of CH_4 (for simplicity only one scenario is presented in Figure 4.14 explicitly). C-D activation of benzene-d_6, followed by a reverse metalation process that transfers deuterium into the [Ph_2BP_2] ligand, ultimately leads to the phenyl platinum complex. **Path D** thus accounts for the high degree of CH_4 released by **3.11** in benzene-d_6 and the incorporation of deuteride into the [Ph_2BP_2] ligand. We explicitly invoke platinum(IV) intermediates along both **Path C** and **Path D** that arise from oxidative addition of benzene-d_6 on the basis of our spectroscopic evidence for a platinum(IV) species resulting from [Ph_2BP_2] metalation (product **B**, **Path B**). Also, we emphasize that our inability to detect the platinum(IV) hydride species produced by [Ph_2BP_2] metalation along **Path D** is because the ligand metalation process is itself rate-determining. Recall a key piece of evidence that supports this assertion: in both benzene and benzene-d_6, *the rate of decay of the d_{20}-labeled derivative*

*$[Ph_2B(CH_2P(C_6D_5)_2)_2]Pt(Me)(THF)$ (**3.11-d_{20}**) is slower than that of $[Ph_2BP_2]Pt(Me)(THF)$ (**3.11**) itself* ($k_{\mathbf{3.11}}/k_{\mathbf{3.11}\text{-}d_{20}} \approx 3$ in benzene-d_6). Under conditions in which **Path D** dominates and ligand metalation is rate-determining, this is just what we expect.

The observation that the rate of decay of $[Ph_2B(CH_2P(C_6D_5)_2)_2]Pt(Me)(THF)$ (**3.11-d_{20}**) is modestly slower in benzene-d_6 than in protio benzene (for **3.11-d_{20}**, $k(C_6H_6)/k(C_6D_6) \approx 1.8$) is perhaps more curious, but can be explained as follows: deuteration of the aryl positions of the $[Ph_2BP_2]$ ligand slows the rate of ligand metalation, and thereby attenuates the overall rate by which **3.11-d_{20}** traverses down **Path D**. This in turn funnels more of the system down **Path C**, a path insensitive to arylphosphine deuteration. In this manner, a pre-equilibrium shift in benzene-d_6 serves to amplify the primary kinetic isotope effect of **Path C** and thereby expose C-H activation as rate-determining along this path as well. *We can therefore suggest that a C-H activation process of some sort is rate-determining for each of the pathways that are outlined in Figure 4.14.*

The final task we are left with is to account for the large role that the $[Ph_2BP_2]$ ligand plays in the solution chemistry of neutral $[Ph_2BP_2]Pt(Me)(THF)$ (**3.11**), whereas the Ph_2SiP_2 ligand appears to be far more innocent with respect to the solution chemistry of cationic $[(Ph_2SiP_2)Pt(Me)(THF)]^+$ (**3.26**). The key distinction between the two ligands is the propensity for the $[Ph_2BP_2]$ ligand to achieve an η^3-binding mode, a binding mode that is less prevalent for the neutral ligand Ph_2SiP_2. Because each ligand is sterically very similar, we commit ourselves to an electronic explanation based upon the more electron-rich nature of **3.11** relative to **3.26**. It seems reasonable to suggest that some of the

anionic borate charge is disseminated to the aryl groups of the [Ph_2BP_2] ligand. This results in aryl groups in the [Ph_2BP_2] ligand that are better electron-pair donors than the aryl groups of the neutral Ph_2SiP_2 ligand. Therefore, although benzene out-competes the aryl donors of the Ph_2SiP_2 ligand with respect to coordinating platinum, thereby leading to the intermolecular solution chemistry observed, benzene does not out-compete the aryl groups of the [Ph_2BP_2] ligand, and intramolecular processes become prevalent. This subtle electronic distinction might thereby bias the overall mechanistic pathways between the neutral and cationic systems.

The propensity for a structurally related neutral and cationic platinum(II) system to mediate intermolecular benzene C-H activation is generally comparable. However, the operational mechanism by which each system mediates this chemistry is distinct. The mechanism by which substrate coordination occurs, and the propensity for intramolecular ligand C-H activation processes, is clearly different between the neutral and cationic systems. This study, along with several others, now allows us to conclude that zwitterions of the type described herein are generally capable of undergoing organometallic reactions akin to their cationic cousins. However, understanding the detailed mechanisms by which these zwitterions mediate elementary reaction transformations will help to define a unique and complementary role for zwitterionic catalysts.

4.4. Experimental section

4.4.1. General considerations

Unless otherwise noted, general procedures were performed according to Section 2.4.1.

4.4.2. Starting materials and reagents

(COD)$PtCl_2$,[25] (COD)PtMeCl, (COD)$Pt(^{13}CH_3)_2$, (COD)PtMePh,[26] (COD)$PtPh_2$,[27] Ph_2PCH_2Li(TMEDA),[28] $[Li(OEt_2)_2][B(C_6F_5)_4]$,[29] $[H(OEt_2)_2][B(C_6F_5)_4]$, $[^nBu_4N][B(C_6F_5)_4]$,[30] (dppp)$PtMe_2$ (**3.25**)[31,32] and $P(C_6F_5)_3$[33] were prepared by literature methods. (dppp)$PtPh_2$ (**4.4**) was prepared by reaction of (COD)$PtPh_2$ with dppp in THF solution. $B(C_6F_5)_3$ was purchased from Aldrich and recrystallized from a filtered pentane solution at -35 ºC prior to use. The ligand $[Ph_2BP_2]$[ASN] (**2.25**[ASN]) and the compounds $[HNEt_3][BPh_4]$, $[HNEt^iPr_2][BPh_4]$,[34] and $Me_3P{=}S$ were prepared as described in Chapter 2. The ligand Ph_2SiP_2 (**3.22**) and the complexes $[[Ph_2BP_2]Pt(Me)_2]$[ASN] (**3.1**), $[Ph_2BP_2]Pt(Me)(THF)$ (**3.11**), $(Ph_2SiP_2)PtMe_2$ (**3.24**), $[(Ph_2SiP_2)Pt(Me)(THF)][B(C_6F_5)_4]$ (**3.26**), and $[(dppp)Pt(Me)(THF)][B(C_6F_5)_4]$ (**3.27**) were prepared as described in Chapter 3.

4.4.3. Syntheses of compounds

$[[Ph_2BP_2]Pt(Me)(Ph)]$[ASN] (4.1). A THF solution (1 mL) of (COD)Pt(Me)(Ph) (70.6 mg, 0.179 mmol) was added to a stirring suspension of $[Ph_2BP_2]$[ASN] (123.1 mg, 0.1785 mmol) in THF (2 mL). The reaction was stirred for 30 min and became homogeneous. The solution was concentrated under reduced pressure, and off-white solids were precipitated with diethyl ether (2 mL). The supernatant was removed, and the solids were washed with ethanol (2 x 2 mL) and diethyl ether (2 x 2 mL) and dried under reduced pressure, producing off-white **4.1** (122.4 mg, 70.2%).

^{1}H NMR (300 MHz, acetone-d_6): δ 7.47 (m, 4H), 7.24 (m, 4H), 7.12 (m, 2H), 7.09 (m, 4H), 6.98 (m, 4H), 6.87 (m, 8H), 6.62 (m, 4H), 6.57 (m, 2H), 6.43 (m, 2H), 6.29 (m, 1H), 3.69 (m, 8H, $((CH_2CH_2)_2)_2N$), 2.26 (m, 8H, $((CH_2CH_2)_2)_2N$), 2.10 (br, 2H,

$Ph_2B(CH_2PPh_2)_2$), 2.02 (br, 2H, $Ph_2B(CH_2PPh_2)_2$), 0.08 (dd, 3H, Pt-CH_3, $^3J_{P\text{-}H(cis)}$ = 6.9 Hz, $^3J_{P\text{-}H(trans)}$ = 7.8 Hz, $^2J_{Pt\text{-}H}$ = 69 Hz). $^{13}C\{^1H\}$ NMR (125.7 MHz, acetone-d_6): δ 166 (br, *ipso* $B(C_6H_5)_2$), 144, 140.5 (d), 139.8 (d), 138.7, 135.0 (m), 134.7 (m), 133.8, 128.9, 128.4, 127.9 (d), 127.5 (d), 127.0, 126.8, 122.4, 120.0, 64.3 $(((CH_2CH_2)_2)_2N)$, 23.3 $(((CH_2CH_2)_2)_2N)$, 23 (br, $Ph_2B(CH_2PPh_2)_2$), 22 (br, $Ph_2B(CH_2PPh_2)_2$), 5.5 (dd, Pt-CH_3, $^2J_{P\text{-}C(trans)}$ = 93 Hz). $^{31}P\{^1H\}$ NMR (121.4 MHz, acetone-d_6): δ 18.3 (d, $^1J_{Pt\text{-}P}$ = 1775 Hz, $^2J_{P\text{-}P}$ = 19 Hz), 17.29 (d, $^1J_{Pt\text{-}P}$ = 1868 Hz, $^2J_{P\text{-}P}$ = 19 Hz). $^{11}B\{^1H\}$ NMR (128.3 MHz, acetone-d_6): δ -13.8. Anal. Calcd. for $C_{53}H_{57}BNP_2Pt$: C, 65.16; H, 5.98; N, 1.43. Found: C, 64.90; H, 6.05; N, 1.54.

[Ph_2BP_2]Pt(Ph)$_2$][ASN] (4.2). A THF solution (2 mL) of (COD)$PtPh_2$ (45.5 mg, 99.5 μmol) was added to a stirring suspension of [Ph_2BP_2][ASN] (68.6 mg, 99.5 μmol) in THF (3 mL). The reaction was stirred for 1 h, during which the mixture became a homogeneous solution. The solution was concentrated and triturated under pentane (3 x 2 mL). The resulting off-white solids were dried under reduced pressure, providing **4.2** (101.0 mg, 97.7%).

^1H NMR (300 MHz, CD_3CN): δ 7.21 (m, 8H), 7.01 (m, 4H), 6.90 (m, 12H), 6.80 (m, 4H), 6.60 (m, 4H), 6.53 (m, 2H), 6.30 (m, 4H), 6.18 (m, 2H), 3.28 (m, 8H, $((CH_2CH_2)_2)_2N$), 2.08 (m, 8H, $((CH_2CH_2)_2)_2N$), 2.02 (br, 4H, $Ph_2B(CH_2PPh_2)_2$). $^{13}C\{^1H\}$ NMR (125.7 MHz, CD_3CN): δ 168.3 (dd, *ipso* Pt$(C_6H_5)_2$, $^2J_{P\text{-}C(trans)}$ = 111 Hz, $^2J_{P\text{-}C(cis)}$ = 12 Hz), 165 (br, *ipso* $B(C_6H_5)_2$), 138.5, 137.4 (s, *ortho* Pt$(C_6H_5)_2$, $^2J_{Pt\text{-}C}$ = 29 Hz), 133.8, 132.4, 127.9, 126.9 (s, *meta* Pt$(C_6H_5)_2$, $^3J_{Pt\text{-}C}$ = 8.9 Hz), 126.2, 126.0, 121.6, 119.4, 63.3 $(((CH_2CH_2)_2)_2N)$, 22.3 $(((CH_2CH_2)_2)_2N$, 20.3 (br, $Ph_2B(CH_2PPh_2)_2$). $^{31}P\{^1H\}$ NMR (121.4 MHz, CD_3CN): δ 13.99 ($^1J_{Pt\text{-}P}$ = 1772 Hz). $^{11}B\{^1H\}$ NMR (128.3 MHz, CD_3CN):

δ -14.4. ES MS: *m/z* 912.3 ([M$^-$]). Anal. Calcd. for $C_{58}H_{60}BNP_2Pt$: C, 67.05; H, 5.82; N, 1.35. Found: C, 66.23; H, 5.96; N, 1.48.

(Ph_2SiP_2)$PtPh_2$ (4.3). Solid Ph_2SiP_2 (70.3 mg, 0.121 mmol) and (COD)$PtPh_2$ (55.4 mg, 0.121 mmol) were dissolved in THF (2 mL). After 20 min, volatiles were removed under reduced pressure. The resulting solids were triturated under petroleum ether (3 mL), and the solution was decanted. The resulting off-white solids were dried under reduced pressure, providing **4.3** (103.2 mg, 91.7%).

^{1}H NMR (300 MHz, $CDCl_3$): δ 7.36 (m, 8H), 7.18 (m, 6H), 7.05 (m, 12 H), 6.93 (m, 4H), 6.87 (m, 4H), 6.44 (m, 4H), 6.31 (m, 2H), 2.41 (d, 4H, $Ph_2Si(CH_2PPh_2)_2$, $^2J_{P\text{-}H}$ = 9.6 Hz, $^3J_{Pt\text{-}H}$ = 33 Hz). $^{13}C\{^1H\}$ NMR (125.7 MHz, $CDCl_3$): δ 162.7 (dd, *ipso* $Pt(C_6H_5)_2$, $^2J_{P\text{-}C}$ = 12, 113 Hz), 136.1 ($J_{Pt\text{-}C}$ = 31 Hz), 135.2, 133.7, 133.3 (m), 129.7, 127.9, 127.8 (m), 126.8 ($J_{Pt\text{-}C}$ = 66 Hz), 120.3, 9.7 (m, $Ph_2Si(CH_2PPh_2)_2$). $^{31}P\{^1H\}$ NMR (121.4 MHz, $CDCl_3$): δ 6.02 ($^1J_{Pt\text{-}P}$ = 1720 Hz). Anal. Calcd. for $C_{50}H_{44}P_2PtSi$: C, 64.57; H, 4.77. Found: C, 64.73; H, 5.12.

[Ph_2BP_2]Pt(Ph)(THF) (4.5). (a) Solid [Ph_2BP_2]Pt(Me)(Ph)[ASN] (23.6 mg, 24.2 μmol) was dissolved in THF (2 mL). While stirring, solid $B(C_6F_5)_3$ (12.5 mg, 24.4 μmol) was added. After 10 min, $^{31}P\{^1H\}$ NMR spectroscopic analysis showed the formation of one major product, consistent with the formulation of **4.5** (see (b)).

(b) Solid [[Ph_2BP_2]$Pt(Ph)_2$][ASN] (51.4 mg, 52.6 μmol) was dissolved in THF (2 mL). A THF solution (2 mL) of [^{i}Pr$_2$EtNH][BPh_4] (23.5 mg, 52.3 μmol) was added to the stirring solution. The clear, colorless reaction slowly produced a white precipitate. The mixture was stirred for 1 h, and the white solids were filtered away. The solution was concentrated under reduced pressure, and pentane (2 mL) was added, precipitating

white solids. The solids were collected by filtration. NMR spectroscopic analysis of the solids was consistent with the formulation of **4.5** as the major product (approximately 80%). Due to the lability of the coordinated THF molecule, obtaining satisfactory combustion analysis was problematic.

^{1}H NMR (300 MHz, C_6D_6): δ 7.56 (m, 4H), 7.46 (m, 4H), 7.21 (m, 4H), 6.95 (m, 18H), 6.88 (m, 2H), 6.78 (m, 2H), 6.73 (m, 1H, *para* Pt-C_6H_5), 2.87 (br, 4H, $(CH_2CH_2)_2O$), 2.64 (br d, 2H, $Ph_2B(CH_2PPh_2)_2$, $^{2}J_{P\text{-}H}$ = 17 Hz), 2.42 (br d, 2H, $Ph_2B(CH_2PPh_2)_2$, $^{2}J_{P\text{-}H}$ = 14 Hz), 0.46 (br, 4H, $(CH_2CH_2)_2O$). $^{13}C\{^{1}H\}$ NMR (125.7 MHz, THF): δ 161 (br, *ipso* $B(C_6H_5)_2$), 136.3, 135.4 (d), 133.0 (d), 132.9 (d), 132.1 (d), 131.5, 129.2, 129.1, 127.6 (d), 126.9 (d), 126.4 (d), 125.5, 122.6, 121.2, 67 ($(CH_2CH_2)_2O$), 26 ($(CH_2CH_2)_2O$), 21 (br, $Ph_2B(CH_2PPh_2)_2$), 17 (br, $Ph_2B(CH_2PPh_2)_2$). $^{31}P\{^{1}H\}$ NMR (121.4 MHz, THF): δ 28.60 ($^{1}J_{Pt\text{-}P}$ = 1740 Hz, $^{2}J_{P\text{-}P}$ = 23 Hz), 11.20 ($^{1}J_{Pt\text{-}P}$ = 4393 Hz, $^{2}J_{P\text{-}P}$ = 23 Hz). $^{11}B\{^{1}H\}$ NMR (128.3 MHz, THF): δ -14.9.

$[(Ph_2SiP_2)Pt(Ph)(THF)][B(C_6F_5)_4]$ (4.6). Solid white $(Ph_2SiP_2)PtPh_2$ (29.3 mg, 31.5 μmol) was dissolved in dichloromethane (2 mL) with THF (0.5 mL). Separately, $[H(OEt_2)_2][B(C_6F_5)_4]$ (25.8 mg, 31.5 μmol) was dissolved in dichloromethane (2 mL) and added slowly to the stirring solution of $(Ph_2SiP_2)PtPh_2$. After addition was complete, the reaction was stirred for 10 min. Volatiles were removed under reduced pressure, and the mixture was triturated and washed using petroleum ether (2 x 2 mL). The resulting white solids were dried under reduced pressure, providing off-white **4.6** (49.2 mg, 97.4%).

^{1}H NMR (500 MHz, CD_2Cl_2): δ 6.4-7.8 (35H, aryl protons), 3.24 (m, 4H, $(CH_2CH_2)_2O$), 2.58 (dd, 2H, $Ph_2Si(CH_2PPh_2)_2$, $J_{P\text{-}H}$ = 3.0, 15.5 Hz, $^{3}J_{Pt\text{-}H}$ = 80 Hz), 2.43 (dd, 2H, $Ph_2Si(CH_2PPh_2)_2$, $^{1}J_{P\text{-}H}$ = 12.5 Hz, $^{3}J_{Pt\text{-}H}$ = 94 Hz), 1.15 (m, 4H, $(CH_2CH_2)_2O$).

$^{13}C\{^{1}H\}$ NMR (125.7 MHz, CD_2Cl_2): δ 159 (d, *ipso* Pt(C_6H_5)), 149.7, 147.8, 139.8, 137.9, 135.8, 128-134, 125.0, 124.3, 68.9 ($CH_2CH_2)_2O$), 24.5 ($CH_2CH_2)_2O$), 12.1 (m, $Ph_2Si(CH_2PPh_2)_2$), 8.3 (m, $Ph_2Si(CH_2PPh_2)_2$). $^{31}P\{^{1}H\}$ NMR (121.4 MHz, CD_2Cl_2): δ 21.0 (d, $^{2}J_{P\text{-}P}$ = 17.1 Hz, $^{1}J_{Pt\text{-}P}$ = 1746 Hz), 0.2 (d, $^{2}J_{P\text{-}P}$ = 17.1 Hz, $^{1}J_{Pt\text{-}P}$ = 4645 Hz). $^{19}F\{^{1}H\}$ NMR (282.1 MHz, CD_2Cl_2): δ -133.5, -163.9, -167.7. $^{11}B\{^{1}H\}$ NMR (128.3 MHz, CD_2Cl_2): δ -18.4. Anal. Calcd. for $C_{72}H_{47}BF_{20}OP_2PtSi$: C, 53.91; H, 2.95. Found: C, 53.55; H, 3.26.

[(dppp)Pt(Ph)(THF)][B(C_6F_5)$_4$] (4.7). Solid white (dppp)$PtPh_2$ (32.1 mg, 42.1 μmol) was dissolved in dichloromethane (2 mL) with THF (0.5 mL). Separately, [H(OEt_2)$_2$][B(C_6F_5)$_4$] (34.5 mg, 42.2 μmol) was dissolved in dichloromethane (2 mL) and added slowly to the stirring solution of (dppp)$PtPh_2$. After addition was complete, the reaction was stirred for 10 min. Volatiles were removed under reduced pressure, and the mixture was triturated and washed using petroleum ether (2 x 2 mL). The resulting white solids were dried under reduced pressure, providing off-white **4.7** (54.0 mg, 89.3%).

^{1}H NMR (300 MHz, CD_2Cl_2): δ 7.7 (m, 4H), 7.6 (m, 6H), 7.4 (m, 6H), 7.3 (m, 6H), 7.0 (m, 2H), 6.7 (m, 3H), 3.33 (m, 4H, ($CH_2CH_2)_2O$), 2.75 (m, 4H, $Ph_2PCH_2CH_2CH_2PPh_2$), 1.7 (m, 2H, $Ph_2PCH_2CH_2CH_2PPh_2$), 1.18 (m, 4H, ($CH_2CH_2)_2O$). $^{13}C\{^{1}H\}$ NMR (125.7 MHz, CD_2Cl_2): δ 158.9 (dd, *ipso* Pt(C_6H_5)), 149.7, 147.8, 139.8, 137.9, 136.0, 133.6 (d), 133.4 (d), 132.4, 130.0 (d), 129.3 (d), 128.5 (d), 125.1, 73.0 (($CH_2CH_2)_2O$), 27.2 (d, $Ph_2PCH_2CH_2CH_2PPh_2$), 27.1 (d, $Ph_2PCH_2CH_2CH_2PPh_2$), 24.6 (($CH_2CH_2)_2O$), 18.6 ($Ph_2PCH_2CH_2CH_2PPh_2$). $^{31}P\{^{1}H\}$ NMR (121.4 MHz, CD_2Cl_2): δ 12.0 (d, $^{2}J_{P\text{-}P}$ = 22.5 Hz, $^{1}J_{Pt\text{-}P}$ = 1620 Hz), -3.0 (d, $^{2}J_{P\text{-}P}$ = 22.5 Hz, $^{1}J_{Pt\text{-}P}$ = 4524 Hz). $^{19}F\{^{1}H\}$ NMR (282.1 MHz, CD_2Cl_2): δ -133.5, -163.9, -167.7. $^{11}B\{^{1}H\}$ NMR (128.3

MHz, CD_2Cl_2): δ -19.1. Anal. Calcd. for $C_{61}H_{39}BF_{20}OP_2Pt$: C, 51.03; H, 2.74. Found: C, 51.21; H, 2.74.

{[Ph_2BP_2]Pt(μ-H)}$_2$ (4.8). Solid [[Ph_2BP_2]Pt($Me)_2$][ASN] (47.2 mg, 51.6 μmol) was suspended in THF (1 mL). Stirring, a THF solution (2 mL) of [HN^iPr_2Et][BPh_4] (23.2 mg, 51.6 μmol) was added. The reaction mixture was stirred for 15 min, then filtered to remove white solids. The solution was concentrated under reduced pressure to approximately 0.25 mL, and petroleum ether (4 mL) was added to precipitate white solids. The white solids were collected by filtration, and dissolved in THF (3 mL). The solution was filtered into a Schlenk flask containing a stirbar, and the flask was sealed with a septum. The flask was flushed with dihydrogen for 10 min while stirring vigorously, causing the solution to become golden yellow. The flask was stirred under a dihydrogen atmosphere for 4 h at ambient temperature. Volatiles were removed under reduced pressure to provide yellow solids. The solids were crystallized from acetone at -35 °C overnight to provide golden crystalline **4.8** (33.0 mg, 84.2%).

^{1}H NMR (300 MHz, acetone-d_6): δ 6.2-7.9 (aryl protons, 60H), 1.97 (br, 8H, $Ph_2B(CH_2PPh_2)_2$), -3.62 ("quintet of quintets", 2H, Pt(μ-*H*), $^1J_{Pt\text{-}H}$ = 461 Hz, $^2J_{P\text{-}H}$ = 40 Hz). $^{31}P\{^1H\}$ NMR (121.4 MHz, acetone-d_6): δ 35.23 ($J_{Pt\text{-}P}$ = 186, 2851 Hz). IR (CH_2Cl_2, KBr): $\nu_{Pt\text{-}H}$ = 1702 cm^{-1}. Anal. Calcd. for $C_{72}H_{70}B_2P_4Pt_2$: C, 60.09; H, 4.64. Found: C, 60.10; H, 4.80.

[{(Ph_2SiP_2)Pt}$_2$(μ-η^3:η^3-biphenyl)][$B(C_6F_5)_4$]$_2$ (4.9). Thermolysis of **3.26** (24.5 mg, 15.9 μmol) in benzene at 55 ºC for 24 h resulted in the formation a single product as evidenced by $^{31}P\{^1H\}$ NMR spectroscopy. Isolation of orange solids by removal of volatiles under reduced pressure followed by washing with petroleum ether (2 x 2 mL)

provided **4.9** (21.7 mg, 89.1%). Crystals of **4.9** were obtained by slow cooling of a saturated solution of **4.9** in *o*-xylene.

^{1}H NMR (300 MHz, acetone-d_6): δ 7.77 (m, 1H), 7.49 (m, 16H), 7.27 (m, 28H), 7.15 (m, 2H), 7.10 (m, 8H), 6.92 (m, 8H), 6.54 (d, 2H), 5.64 (m, 1H), 4.24 (br d, 2H), 4.03 (br t, 2H), 2.73 (d, 8H, $Ph_2Si(CH_2PPh_2)_2$, $^{2}J_{P\text{-}H}$ = 13.2 Hz, $^{3}J_{Pt\text{-}H}$ = 62.4 Hz). ^{13}C{^{1}H} NMR (125.7 MHz, acetone-d_6): δ 150.6, 148.7, 140.6, 138.7, 135.1, 134.1, 133.6, 132.9, 130.5, 129.3, 126.5, 107.4, 95.7, 81.2, 76.1, 9.3 (br, $Ph_2Si(CH_2PPh_2)_2$). ^{31}P{^{1}H} NMR (121.4 MHz, acetone-d_6): δ 8.42 ($^{1}J_{Pt\text{-}P}$ = 3940 Hz). ^{19}F{^{1}H} NMR (282.1 MHz, acetone-d_6): δ -132.5, -163.6 (t), -167.6. ES MS: *m/z* 852.8 ([M^{++}]). Anal. Calcd. for $C_{136}H_{78}B_2F_{40}P_4Pt_2Si_2$: C, 53.31; H, 2.57. Found: C, 51.82; H, 2.35.

[{(dppp)Pt}$_2$(μ-η^3:η^3-biphenyl)][B(C$_6$F$_5$)$_4$]$_2$ (4.10). Thermolysis of **4.7** (32.7 mg, 22.8 μmol) in benzene at 55 ºC for 4 h resulted in the formation of two products as evidenced by ^{31}P{^{1}H} NMR spectroscopy. Removal of volatiles under reduced pressure provided a mixture of **4.10** and a second species which is presumed to be the hydroxy-bridged dimer, $[(dppp)Pt(\mu\text{-}OH)]_2[B(C_6F_5)_4]_2$. Spectral analysis was consistent with the formulation of the major product as **4.10** by comparison to **4.9** and previously reported systems.

^{1}H NMR (300 MHz, CD_2Cl_2): δ 6.6-7.8 (aryl protons), 5.15 (m, 1H), 4.21 (br, 2H), 3.67 (br, 2H), 2.63 (br, 8H, $Ph_2PCH_2CH_2CH_2PPh_2$), 1.64 (m, 4H, $Ph_2PCH_2CH_2CH_2PPh_2$). ^{31}P{^{1}H} NMR (121.4 MHz, CD_2Cl_2): δ 0.20 ($^{1}J_{Pt\text{-}P}$ = 3737 Hz). ^{19}F{^{1}H} NMR (282.1 MHz, CD_2Cl_2): δ -133.4, -163.7 (t), -167.5.

[Ph$_2$BP$_2$]Pt(Me)(pyridine) (4.11). Solid [[Ph_2BP_2]Pt(Me)$_2$][ASN] (187.9 mg, 205.4 μmol) was suspended in THF (5 mL). Stirring, a THF solution (4 mL) of

[HN^{i}Pr$_2$Et][BPh$_4$] (92.4 mg, 206 μmol) was added. The reaction mixture was stirred for 15 min, then filtered to remove white solids. Pyridine (20 μL, 250 μmol) was added to the solution. After 15 min, analysis by ^{31}P{^{1}H} NMR spectroscopy showed the formation of a single product. Volatiles were removed from the reaction mixture under reduced pressure. The resulting white solids were washed with petroleum ether (2 x 3 mL), dissolved in benzene (4 mL), and filtered. Removal of volatiles under reduced pressure provided white solids (165.8 mg, 94.7%).

^{1}H NMR (300 MHz, C_6D_6): δ 7.75 (m, 4H), 7.54 (br m, 2H), 7.34 (br d, 4H), 7.25 (t, 4H), 7.08 (m, 12H), 6.89 (t, 2H), 6.79 (t, 4H), 6.30 (t, 1H, *para*-Pt-NC$_5$*H*$_5$), 5.87 (t, 2H), 2.62 (br d, 2H, Ph$_2$B(C*H*$_2$PPh$_2$)$_2$), 2.51 (br d, 2H, Ph$_2$B(C*H*$_2$PPh$_2$)$_2$), 0.45 (dd, 3H, Pt-C*H*$_3$, $^{2}J_{\text{Pt-H}}$ = 56 Hz, $^{3}J_{\text{P-H}}$ = 3.0, 6.9 Hz). ^{31}P{^{1}H} NMR (121.4 MHz, C_6D_6): δ 24.57 (d, $^{1}J_{\text{Pt-P}}$ = 1739 Hz, $^{2}J_{\text{P-P}}$ = 22 Hz), 12.12 (d, $^{1}J_{\text{Pt-P}}$ = 3591 Hz, $^{2}J_{\text{P-P}}$ = 22 Hz).

[Ph$_2$BP$_2$]Pt(Me)(O-*N*-pyridine) (4.12). Solid [[Ph$_2$BP$_2$]Pt(Me)$_2$][ASN] (18.9 mg, 20.7 μmol) was suspended in THF (1 mL). Stirring, a THF solution (2 mL) of [^{i}Pr$_2$EtNH][BPh$_4$] (9.3 mg, 20.7 μmol) was added. The reaction mixture was stirred for 15 min, then filtered to remove white solids. Pyridine-*N*-oxide (2.0 mg, 2.1 μmol) was added to the solution. Volatiles were removed from the reaction mixture under reduced pressure. The resulting white solids were washed with petroleum ether (2 x 3 mL), dissolved in benzene (4 mL), and filtered. Removal of volatiles under reduced pressure provided white solids (16.9 mg, 93.9%).

^{1}H NMR (300 MHz, C_6D_6): δ 7.70 (m, 4H), 7.61 (m, 6H), 7.46 (br d, 4H), 7.08 (m, 4H), 7.03 (m, 8H), 6.92 (m, 4H), 6.09 (br, 1H), 5.97 (t , 2H), 5.75 (t, 2H), 2.66 (br d, 2H, Ph$_2$B(C*H*$_2$PPh$_2$)$_2$), 2.38 (br d, 2H, Ph$_2$B(C*H*$_2$PPh$_2$)$_2$), 0.37 (dd, 3H, Pt-C*H*$_3$, $^{2}J_{\text{Pt-H}}$ =

40 Hz, $^{3}J_{P\text{-}H}$ = 1.5, 6.9 Hz). $^{31}P\{^{1}H\}$ NMR (121.4 MHz, C_6D_6): δ 28.68 (d, $^{1}J_{Pt\text{-}P}$ = 1803 Hz, $^{2}J_{P\text{-}P}$ = 22 Hz), 14.71 (d, $^{1}J_{Pt\text{-}P}$ = 4197 Hz, $^{2}J_{P\text{-}P}$ = 22 Hz).

[Ph$_2$BP$_2$]Pt(Me)(SMe$_2$) (4.13). Solid [[Ph_2BP_2]Pt$(Me)_2$][ASN] (41.0 mg, 44.8 μmol) was suspended in THF (2 mL). Stirring, a THF solution (2 mL) of [$^{i}Pr_2$EtNH][BPh_4] (20.1 mg, 44.7 μmol) was added. The reaction mixture was stirred for 15 min, then filtered to remove white solids. Dimethylsulfide (3.4 μL, 46 μmol) was added to the solution. After 15 min, the reaction mixture was concentrated under reduced pressure to 0.5 mL. Petroleum ether (3 mL) was added, precipitating white solids. The solution was decanted. The resulting white solids were washed with petroleum ether (2 x 3 mL), dissolved in benzene (5 mL), and filtered. Removal of volatiles under reduced pressure provided white solids (34.5 mg, 92.2%).

^{1}H NMR (300 MHz, C_6D_6): δ 7.59 (m, 4H), 7.47 (m, 4H), 7.25 (br d, 4H), 7.01 (m, 16H), 6.80 (m, 2H), 2.63 (br d, 2H, $Ph_2B(CH_2PPh_2)_2$), 2.43 (br d, 2H, $Ph_2B(CH_2PPh_2)_2$), 1.13 (d, 6H, Pt-S$(CH_3)_2$, $^{3}J_{Pt\text{-}H}$ = 34 Hz, $^{4}J_{P\text{-}H}$ = 3.3 Hz), 0.32 (dd, 3H, Pt-CH_3, $^{2}J_{Pt\text{-}H}$ = 54 Hz, $^{3}J_{P\text{-}H}$ = 3.9, 6.9 Hz). $^{31}P\{^{1}H\}$ NMR (121.4 MHz, C_6D_6): δ 22.28 (d, $^{1}J_{Pt\text{-}P}$ = 3572 Hz, $^{2}J_{P\text{-}P}$ = 25 Hz), 19.20 (d, $^{1}J_{Pt\text{-}P}$ = 1753 Hz, $^{2}J_{P\text{-}P}$ = 25 Hz).

[Ph$_2$BP$_2$]Pt(Me)(PMe$_3$) (4.14). Solid [[Ph_2BP_2]Pt$(Me)_2$][ASN] (114.3 mg, 125.0 μmol) was suspended in THF (2 mL). Stirring, a THF solution (2 mL) of [$^{i}Pr_2$EtNH][BPh_4] (56.3 mg, 125 μmol) was added. The reaction mixture was stirred for 15 min, then filtered to remove white solids. Trimethylphosphine (13.4 μL, 129 μmol) was added to the solution. After 15 min, volatiles were removed from the reaction mixture under reduced pressure. The resulting white solids were washed with petroleum

ether (2 x 3 mL), dissolved in a benzene/THF mixture (6 mL : 1 mL), and filtered. Removal of volatiles under reduced pressure provided white solids (106.0 mg, 99.9%).

$^{31}P\{^{1}H\}$ NMR (121.4 MHz, THF): δ 24.30 (dd, $^{2}J_{P\text{-}P}$ = 28.0, 389 Hz, $^{1}J_{Pt\text{-}P}$ = 2611 Hz), 15.22 (br, $^{1}J_{Pt\text{-}P}$ = 1854 Hz), -18.09 (br d, $^{2}J_{P\text{-}P}$ = 389 Hz, $^{1}J_{Pt\text{-}P}$ = 2469 Hz).

[Ph_2BP_2]Pt(Me)($S{=}PMe_3$) (4.15). Solid [[Ph_2BP_2]Pt$(Me)_2$][ASN] (98.5 mg, 0.108 mmol) and [$^{i}Pr_2EtNH$][BPh_4] (48.5 mg, 0.108 mmol) were combined and THF (3 mL) was added. The reaction mixture was stirred for 15 min. The reaction mixture was filtered into a vial containing solid $Me_3P{=}S$ (11.7 mg, 0.108 mmol). The resulting solution was stirred for 10 min, and then volatiles were removed under reduced pressure. The solids were dissolved in benzene (2 mL), filtered, and lyophilized, providing analytically pure white solids (94.2 mg, 98.9%).

^{1}H NMR (300 MHz, C_6D_6): δ 7.61 (m, 8H), 7.34 (br d, 4H), 7.05 (m, 12H), 6.97 (m, 6H), 2.71 (br d, 2H, $Ph_2B(CH_2PPh_2)_2$, $^{2}J_{P\text{-}H}$ = 16 Hz, $^{3}J_{Pt\text{-}H}$ = 77 Hz), 2.41 (br d, 2H, $Ph_2B(CH_2PPh_2)_2$, $^{2}J_{P\text{-}H}$ = 14 Hz, $^{3}J_{Pt\text{-}H}$ = 59 Hz), 0.60 (d, 9H, Pt-S=$P(CH_3)_3$, $^{2}J_{P\text{-}H}$ = 14 Hz), 0.55 (dd, 3H, Pt-CH_3, $^{2}J_{Pt\text{-}H}$ = 57 Hz, $^{3}J_{P\text{-}H}$ = 4.3, 6.6 Hz). $^{31}P\{^{1}H\}$ NMR (121.4 MHz, C_6D_6): δ 35.26 (dd, $^{2}J_{Pt\text{-}P}$ = 59 Hz, $^{3}J_{P\text{-}P}$ = 9.2, 12 Hz), 23.28 (dd, $^{1}J_{Pt\text{-}P}$ = 3857 Hz, $J_{P\text{-}P}$ = 9.2, 23 Hz), 19.59 (dd, $^{1}J_{Pt\text{-}P}$ = 1721 Hz, $J_{P\text{-}P}$ = 13, 23 Hz). $^{11}B\{^{1}H\}$ NMR (128.3 MHz, C_6D_6): δ -14.4. Anal. Calcd. for $C_{42}H_{46}BP_3PtS$: C, 57.21; H, 5.26. Found: C, 56.87; H, 5.47.

[Ph_2BP_2]Pt(Me){$P(C_6F_5)_3$} (4.16). A THF solution (2 mL) of **3.11** (104.5 mg, 123.6 μmol) was added to solid $P(C_6F_5)_3$ (66.1 mg, 124.2 μmol). The resulting solution was concentrated under reduced pressure. Toluene (4 mL) was added, and the solution was concentrated under reduced pressure. Petroleum ether (2 mL) was added, forming a

white precipitate, which was collected by filtration and washed with additional petroleum ether (2 mL). The solids were dissolved in benzene (2 mL), and the solution was filtered. Volatiles were removed under reduced pressure, providing white solid **4.16** (133.2 mg, 82.5%). Crystals suitable for X-ray diffraction were grown from petroleum ether diffusion into a benzene solution of **4.16**.

^{1}H NMR (300 MHz, C_6D_6): δ 7.44 (br, 4H), 7.26-7.30 (br, 8H), 7.06 (m, 6H), 6.93 (br, 6H), 6.81 (br, 6H), 2.63 (br d, 2H, $Ph_2B(CH_2PPh_2)_2$, $^{2}J_{P\text{-}H}$ = 15 Hz, $^{3}J_{Pt\text{-}H}$ = 53 Hz), 2.24 (dd, 2H, $Ph_2B(CH_2PPh_2)_2$, $^{2}J_{P\text{-}H}$ = 10, 14 Hz, $^{3}J_{Pt\text{-}H}$ = 59 Hz), 0.04 (ddd, 3H, Pt-CH_3, $^{3}J_{P\text{-}H}$ = 5.4, 5.4, 11 Hz, $^{2}J_{Pt\text{-}H}$ = 54 Hz). ^{13}C{^{1}H} NMR (125.7 MHz, C_6D_6): δ 163 (br, *ipso* $B(C_6H_5)_2$), 148.3, 146.2, 145.1, 143.0, 138.9, 136.9, 133.9, 132.8, 130.2, 129.9, 128, 127.1, 123.1, 103.6, 23.4 (br, $Ph_2B(CH_2PPh_2)_2$), 19.8 (br, $Ph_2B(CH_2PPh_2)_2$), 0.75 (br d, Pt-CH_3, $^{1}J_{Pt\text{-}C}$ = 500 Hz, $^{2}J_{P\text{-}C(trans)}$ = 69 Hz). ^{31}P{^{1}H} NMR (121.4 MHz, C_6D_6): δ 22.83 (dd, $^{1}J_{Pt\text{-}P}$ = 3139 Hz, $^{2}J_{P\text{-}P}$ = 29.9, 433 Hz), 18.84 (dd, $^{1}J_{Pt\text{-}P}$ = 1945 Hz, $^{2}J_{P\text{-}P}$ = 17.1, 29.2 Hz), -17.97 (br d, $^{1}J_{Pt\text{-}P}$ = 2499 Hz, $^{2}J_{P\text{-}P}$ = 430 Hz). ^{11}B{^{1}H} NMR (128.3 MHz, C_6D_6): δ -19.1. ^{19}F{^{1}H} NMR (282.1 MHz, C_6D_6): δ -124.5 (br sh), -127.0 (br), -135.2 (br), -145.4 (br), -155.4 (br sh), -157.6 (br), -159.6 (br). Anal. Calcd. for $C_{57}H_{37}BF_{15}P_3Pt$: C, 52.43; H, 2.86. Found: C, 52.51; H, 2.63.

$[Ph_2BP_2]Pt(Ph)\{P(C_6F_5)_3\}$ (4.17). Thermolysis of **4.16** (43.2 mg) in benzene (0.7 mL) at 80 ºC over 24 h led to the quantitative formation of **4.17**.

^{1}H NMR (300 MHz, C_6D_6): δ 6.2-7.8 (35H, aryl protons), 2.0-2.8 (br, 4H, $Ph_2B(CH_2PPh_2)_2$). ^{31}P{^{1}H} NMR (121.4 MHz, C_6D_6): δ 17.92 (dd, $^{2}J_{P\text{-}P}$ = 28, 419 Hz, $^{1}J_{Pt\text{-}P}$ = 3132 Hz), 10.85 (br m, $^{1}J_{Pt\text{-}P}$ = 1770 Hz), -24.01 (br d, $^{2}J_{P\text{-}P}$ = 422 Hz, $^{1}J_{Pt\text{-}P}$ = 2462 Hz). ^{11}B{^{1}H} NMR (128.3 MHz, C_6D_6): δ -15.5. ^{19}F{^{1}H} NMR (282.1 MHz,

C_6D_6): δ -126.4 (br), -129.5 (br), -133.1 (br), -145 (br), -158.3 (br), -160.1 (br). Anal. Calcd. for $C_{62}H_{39}BF_{15}P_3Pt$: C, 54.44; H, 2.87. Found: C, 54.58; H, 2.62.

(Ph_2SiP_2)Pt(Me)(Ph) (4.18). Solid Ph_2SiP_2 (39.7 mg, 68.4 μmol) and (COD)Pt(Me)(Ph) (27.0 mg, 68.3 μmol) were dissolved in THF (2mL) and stirred for 10 min. Volatiles were removed under reduced pressure, and the mixture was triturated with petroleum ether (3 x 3 mL). The resulting off-white solids were dried under reduced pressure to provide **4.18** (52.6 mg, 88.7%).

^{1}H NMR (300 MHz, C_6D_6): δ 7.64 (m, 4H), 7.53 (m, 2H), 7.39 (m, 4H), 7.04 - 6.80 (m, 25H), 2.27 (d, 2H, $Ph_2Si(CH_2PPh_2)_2$, $^2J_{P\text{-}H}$ = 10.8 Hz), 2.19 (d, 2H, $Ph_2Si(CH_2PPh_2)_2$, $^2J_{P\text{-}H}$ = 11.4 Hz), 1.09 (dd, 3H, Pt-CH_3, $^3J_{P\text{-}H}$ = 7.2 Hz, $^3J_{P\text{-}H}$ = 9.6 Hz, $^2J_{Pt\text{-}H}$ = 70 Hz). $^{31}P\{^1H\}$ NMR (121.4 MHz, C_6D_6): δ 8.96 ($^1J_{Pt\text{-}P}$ = 1792 Hz, $^2J_{P\text{-}P}$ = 14 Hz), 8.08 ($^1J_{Pt\text{-}P}$ = 1715 Hz, $^2J_{P\text{-}P}$ = 14 Hz). Anal. Calcd. for $C_{45}H_{42}P_2PtSi$: C, 62.27; H, 4.88. Found: C, 61.47; H, 4.87.

[(Ph_2SiP_2)Pt(Me){$P(C_6F_5)_3$}][$B(C_6F_5)_4$] (4.19). Solid **3.26** (29.0 mg, 18.8 μmol) was dissolved in dichloromethane (2 mL) with $P(C_6F_5)_3$ (10.0 mg, 18.8 μmol) and the solution was stirred for 10 min. Volatiles were removed under reduced pressure. The resulting solids were triturated under toluene (2 mL), washed with petroleum ether (2 x 2 mL), and dried under reduced pressure, providing **4.19** (29.7 mg, 79.0%).

^{1}H NMR (300 MHz, CD_2Cl_2): δ 7.40 (br, 8H), 7.32 (m, 6H), 7.28 (m, 8H), 7.13 (t, 4H), 6.93 (d, 4H), 2.58 (d, 2H, $Ph_2Si(CH_2PPh_2)_2$, $^2J_{P\text{-}H}$ = 12.9 Hz, $^3J_{Pt\text{-}H}$ = 34 Hz), 2.15 (dd, 2H, $Ph_2Si(CH_2PPh_2)_2$, $J_{P\text{-}H}$ = 5.7, 15.0 Hz, $^3J_{Pt\text{-}H}$ = 48 Hz), 0.03 (ddd, 3H, Pt-CH_3, $^3J_{P\text{-}H}$ = 6.6, 10.8, 12.0 Hz, $^2J_{Pt\text{-}H}$ = 51 Hz). $^{13}C\{^1H\}$ NMR (125.7 MHz, CD_2Cl_2): δ 149.7, 148.4, 147.8, 146.4, 143.9, 139.5, 137.9, 135.9, 134.0, 133.8, 132.9, 132.4, 130.9, 129.4,

128.9, 124.3, 102.2, 11.8 (br, $Ph_2Si(CH_2PPh_2)_2$), 9.8 (br, $Ph_2Si(CH_2PPh_2)_2$), 5.8 (m, Pt-CH_3). $^{31}P\{^1H\}$ NMR (121.4 MHz, CD_2Cl_2): δ 13.09 (dd, $^2J_{P\text{-}P}$ = 449, 27.5 Hz, $^1J_{Pt\text{-}P}$ = 3246 Hz), 9.37 (dd, $^2J_{P\text{-}P}$ = 21.4, 27.5 Hz, $^1J_{Pt\text{-}P}$ = 1984 Hz), -19.03 (br d, $^2J_{P\text{-}P}$ = 443 Hz, $^1J_{Pt\text{-}P}$ = 2796 Hz). $^{19}F\{^1H\}$ NMR (282.1 MHz, CD_2Cl_2): δ -126.9 (br), -133.7, -143.7 (br), -157.7 (br), -163.9, -167.8. Anal. Calcd. for $C_{81}H_{37}BF_{35}P_3PtSi$: C, 48.59; H, 1.86. Found: C, 46.88; H, 2.09.

$[(Ph_2SiP_2)Pt(Ph)\{P(C_6F_5)_3\}][B(C_6F_5)_4]$ (4.20). Solid **4.3** (26.5 mg, 28.5 μmol) was dissolved in dichloromethane (1 mL) with $P(C_6F_5)_3$ (15.2 mg, 28.6 μmol). While stirring, a dichloromethane solution (1 mL) of $[H(OEt_2)_2][B(C_6F_5)_4]$ (23.3 mg, 28.5 μmol) was added slowly. After 10 min, volatiles were removed under reduced pressure. The solids were washed with petroleum ether (2 x 2 mL) and dried under reduced pressure (51.4 mg). The resulting solids were comprised of 90-95% **4.20** and 5-10% **4.9**; therefore, elemental analysis was not obtained.

^1H NMR (300 MHz, CD_2Cl_2): δ 7.0-7.6, 6.77 (m), 6.46 (m), 6.23 (br), 2.64 (br, 2H, $Ph_2Si(CH_2PPh_2)_2$), 2.33 (br, 2H, $Ph_2Si(CH_2PPh_2)_2$). $^{31}P\{^1H\}$ NMR (121.4 MHz, CD_2Cl_2): δ 6.79 (dd, $^2J_{P\text{-}P}$ = 25, 445 Hz, $^1J_{Pt\text{-}P}$ = 3319 Hz), 3.04 (dd, $^2J_{P\text{-}P}$ = 19, 25 Hz, $^1J_{Pt\text{-}P}$ = 1870 Hz), 26.61 (dd, $^2J_{P\text{-}P}$ = 19, 440 Hz, $1J_{Pt\text{-}P}$ = 2785 Hz). $^{19}F\{^1H\}$ NMR (282 MHz, CD_2Cl_2): δ -124.3 (br), -133.5, -144.1 (br), -158.2 (br), -163.9, -167.8.

$MeP(C_6D_5)_2$ (4.21). C_6D_5Br (10.0533 g, 62.034 mmol) was reacted with Mg^0 (3.033 g, 124.8 mmol) in Et_2O at reflux over 2 h to form the aryl Grignard reagent. The solution was transferred by cannula to a Schlenk flask containing $MePCl_2$ (3.6193 g, 30.953 mmol) in Et_2O (100 mL) at -78 ºC. The reaction was stirred and warmed gradually over 4 h. Volatiles were removed under reduced pressure, and the resulting

sludge was extracted with petroleum ether (100 mL) and filtered. The solution was concentrated under reduced pressure, providing **4.21** (2.702 g, 41%).

^{1}H NMR (300 MHz, $CDCl_3$): δ 1.65 (d, PC*H*$_3$, $^{2}J_{P\text{-}H}$ = 3.3 Hz). $^{31}P\{^{1}H\}$ NMR (121.4 MHz, $CDCl_3$): δ -26.9. GC MS**:** *m/z* 210 ([M^+]).

4.4.4. Kinetic methodology

THF exchange experiments. A weighed amount (≈ 20 mg) of methyl solvento complex **3.11** or **3.26** was dissolved in C_6D_6 with a known concentration (3-15 eq) of THF in a J. Young tube. The temperature of the probe on a Varian Inova 500 spectrometer was equilibrated and determined using the temperature-dependent peak separation of methanol or ethylene glycol. The J. Young tube was inserted into the probe and allowed to thermally equilibrate. The 90º pulse width of the peak to be inverted (downfield peak of free THF, approx. 3.6 ppm) was determined before each experiment at the appropriate temperature. Magnetization transfer experiments were performed using the DANTE pulse sequence by selectively inverting the downfield free THF peak. The peak areas for free and bound THF were measured after different pulse-mixing times (30 μsec to 50 sec) using a non-selective 90º pulse. Between 25 and 40 data points were acquired as four repetitions with a 50 second relaxation delay. The rate of exchange was determined using the CIFIT computer program.

Kinetics experiments. In a typical experiment, 20-30 mg of the appropriate methyl solvento complex (**3.11**, **3.26**, or **3.27**) or methyl phosphine complex (**4.16** or **4.19**) (and when appropriate, [$^{n}Bu_4N$][$B(C_6F_5)_4$], THF, or $P(C_6F_5)_3$) was dissolved in C_6H_6 or C_6D_6 (0.64 mL) and filtered into a J. Young tube holding a capillary containing an internal integration standard (PMe_3 ($^{31}P\{^{1}H\}$ NMR) or Cp_2Fe (^{1}H NMR) in C_6D_6).

The sealed tube was then heated in a temperature-equilibrated heating block or in the NMR probe. Heating block temperature was calibrated using a thermocouple device, and NMR probe temperature was calibrated using an ethylene glycol standard. The reaction was monitored either by $^{31}P\{^{1}H\}$ NMR and integrating the most downfield peak (corresponding to the ligated phosphorus atom *trans* to the methyl ligand in each case) versus the internal standard (PMe_3), or by ^{1}H NMR and integrating the peak corresponding to the methyl ligand versus the internal standard (Cp_2Fe). The resulting data was fit to a pseudo-first-order decay of the methyl solvento species. Each experiment was repeated in triplicate. The values of the rate constants are an average of three experimental results, and the errors reported are the standard deviation of the three observed rate constants.

4.4.5. X-ray experimental information

The general X-ray experimental procedure was performed according to section 2.4.4. Crystallographic information is provided in Table 4.4.

Table 4.4. X-ray diffraction experimental details for **4.8**, **4.9·4(*o*-xylene)**, and **4.16·C_6H_6**.

	4.8	**4.9·4(*o*-xylene)**	**4.16·C_6H_6**
CCDC ID	238121	186231	198490
Chemical formula	$C_{76}H_{68}B_2P_4Pt_2$	$[C_{88}H_{78}P_4Si_2Pt_2][B(C_6F_5)_4]_2 \cdot 4(C_8H_{10})$	$C_{57}H_{37}BF_{15}P_3Pt \cdot C_6H_6$
Formula weight	1516.98	3063.81 · 4(106.17)	1305.67 · 78.11
T (ºC)	-175	-175	-175
λ (Å)	0.71073	0.71073	0.71073
a (Å)	11.337(3)	15.3609(8)	11.096(2)
b (Å)	12.497(3)	17.3619(9)	12.329(3)
c (Å)	13.007(3)	32.539(2)	20.719(4)
α (º)	68.332(3)	93.281(1)	96.85(3)
β (º)	84.307(4)	95.378(1)	103.38(3)
γ (º)	70.829(4)	105.286(1)	92.92(3)
V (Å^3)	1617.1(7)	8303.7(7)	2728.7(9)
Space group	$P\bar{1}$	$P\bar{1}$	$P\bar{1}$
Z	1	2	2
D_{calcd} (g cm^{-3})	1.558	1.395	1.684
μ (cm^{-1})	44.63	18.29	27.53
*R*1, *wR*2 (I>2σ(I))	0.0324, 0.0616	0.1267, 0.2483	0.0297, 0.0621

$R1 = \Sigma \, | |F_o| - |F_c| | \, / \, \Sigma \, |F_o|$, $wR2 = \{ \Sigma [w(F_o^2 - F_c^2)^2] / \Sigma [w(F_o^2)^2] \}^{1/2}$

References cited

1) For a few examples of cationic metal-mediated bond-forming and polymerization reactions, see: a) Schrock, R. R.; Osborn, J. A. *J. Am. Chem. Soc.* **1971**, *93*, 3089-3091. b) Crabtree, R. H. *Acc. Chem. Res.* **1979**, *12*, 331-337. c) Yasutake, M.; Gridnev, I. D.; Higashi, N.; Imamoto, T. *Org. Lett.* **2001**, *3*, 1701-1704. d) Oi, S.; Terada, E.; Ohuci, K.; Kato, T.; Tachibana, Y.; Inoue, Y. *J. Org. Chem.* **1999**, *64*, 8660-8667. e) Ghosh, A. K.; Matsuda, H. *Org. Lett.* **1999**, *1*, 2157-2159. f) Madine, J. W.; Wang, X.; Widenhoefer, R. A. *Org. Lett.* **2001**, *3*, 385-388. g) LaPointe, A. M.; Rix, F. C.; Brookhart, M. *J. Am. Chem. Soc.* **1997**, *119*, 906-917. h) Beletskaya, I. P.; Cheprakov, A. V. *Chem. Rev.* **2000**, *100*, 3009-3066. i) Ittel, S. D.; Johnson, L. K.; Brookhart, M. *Chem. Rev.* **2000**, *100*, 1169-1203.

2) Recent summaries and examples of cationic metal-mediated C-H bond activation and functionalization include: a) Arndtsen, B. A.; Bergman, R. G.; Mobley, T. A.; Peterson, T. H. *Acc. Chem. Res.* **1995**, *28*, 154-162. b) Lohrenz, J. C. W.; Jacobsen, H. *Angew. Chem., Int. Ed. Engl.* **1996**, *35*, 1305-1307. c) Sen, A. *Acc. Chem. Res.* **1998**, *31*, 550-557. d) Stahl, S. S.; Labinger, J. A.; Bercaw, J. E. *Angew. Chem., Int. Edit.* **1998**, *37*, 2181-2192. e) Balzarek, C.; Weakley, T. J. R.; Tyler, D. R. *J. Am. Chem. Soc.* **2000**, *122*, 9427-9434. f) Tellers, D. M.; Bergman, R. G. *J. Am. Chem. Soc.* **2000**, *122*, 954-955. g) Crabtree, R. H. *J. Chem. Soc., Dalton Trans.* **2001**, 2437-2450. h) Wang, C.; Ziller, J.W.; Flood, T. C. *J. Am. Chem. Soc.* **1995**, *117*, 1647-1648. i) Shilov, A. E.; Shul'pin, G. B. *Activation and Catalytic Reactions of Saturated Hydrocarbons in the Presence of Metal Complexes*; Kluwer: Boston, 2000.

3) a) Thomas, J. C.; Peters, J. C. *J. Am. Chem. Soc.* **2001**, *123*, 5100-5101. b) Lu, C. C.; Peters, J. C. *J. Am. Chem. Soc.* **2002**, *124*, 5272-5273. c) Jenkins, D. M.; Betley, T. A.; Peters, J. C. *J. Am. Chem. Soc.* **2002**, *124*, 11238-11239. d) Jenkins, D. M.; Di Bilio, A. J.; Allen, M. J.; Betley, T. A.; Peters, J. C. *J. Am. Chem. Soc.* **2002**, *124*, 15336-15350. e) Brown, S. D.; Betley, T. A.; Peters, J. C. *J. Am. Chem. Soc.* **2003**, *125*, 322-323. f) Betley, T. A.; Peters, J. C. *Inorg. Chem.* **2002**, *41*, 6541-6543. g) Betley, T. A.; Peters, J. C. *Angew. Chem., Int. Ed.* **2003**, *42*, 2385-2389.

4) a) Hoic, D. A.; Davis, W. M.; Fu, G. C. *J. Am. Chem. Soc.* **1996**, *118*, 8176-8177. b) Seymore, S. B.; Brown, S. N. *Inorg. Chem.* **2000**, *39*, 325-332. c) Padilla-Martínez, I. I.; Poveda, M. L.; Carmona, E.; Monge, M. A.; Ruiz-Valero, C. *Organometallics* **2002**, *21*, 93-104.

5) a) Stahl, S. S.; Labinger, J. A.; Bercaw, J. E. *J. Am. Chem. Soc.* **1995**, *117*, 9371-9372. b) Stahl, S. S.; Labinger, J. A.; Bercaw, J. E. *J. Am. Chem. Soc.* **1996**, *118*, 5961-5976.

6) a) Holtcamp, M. W.; Labinger, J. A.; Bercaw, J. E. *J. Am. Chem. Soc.* **1997**, *119*, 848-849. b) Holtcamp, M. W.; Henling, L. M.; Day, M. W.; Labinger, J. A.; Bercaw, J. E. *Inorg. Chim. Acta* **1998**, *270*, 467-478.

7) Zhong, H. A.; Labinger, J. A.; Bercaw, J. E. *J. Am. Chem. Soc.* **2002**, *124*, 1378-1399.

8) a) Wick, D. D.; Goldberg, K. I. *J. Am. Chem. Soc.* **1997**, *119*, 10235-10236. b) Periana, R. A.; Taube, D. J.; Gamble, S.; Taube, H.; Satoh, T.; Fujii, H. *Science* **1998**, *280*, 560-564. c) Vedernikov, A. N.; Caulton, K. G. *Angew. Chem. Int. Ed.* **2002**, *41*, 4102-4104.

9) a) Johansson, L.; Ryan, O. B.; Tilset, M. *J. Am. Chem. Soc.* **1999**, *121*, 1974-1975. b) Heiberg, H.; Johannson, L.; Gropen, O.; Ryan, O. B.; Swang, O.; Tilset, M. *J. Am. Chem. Soc.* **2000**, *122*, 10831-10845. c) Johansson, L.; Tilset, M.; Labinger, J. A.; Bercaw, J. E. *J. Am. Chem. Soc.* **2000**, *122*, 10846-10855. d) Johannson, L.; Tilset, M. *J. Am. Chem. Soc.* **2001**, *123*, 739-740. e) Johansson, L.; Ryan, O. B.; Rømming, C.; Tilset, M. *J. Am. Chem. Soc.* **2001**, *123*, 6579-6590.

10) a) Reinartz, S.; White, P. S.; Brookhart, M.; Templeton, J. L. *Organometallics* **2001**, *20*, 1709-1712. b) Reinartz, S.; White, P. S.; Brookhart, M.; Templeton, J. L. *J. Am. Chem. Soc.* **2001**, *123*, 12724-12725.

11) Other phosphine-supported platinum(II) systems which have demonstrated C-H bond activation include: a) Brainard, R. L.; Nutt, W. R.; Lee, T. R.; Whitesides, G. M. *Organometallics* **1988**, *7*, 2379-2386. b) Peters, R. G.; White, S.; Roddick, D. M.

Organometallics **1998**, *17*, 4493-4499. c) Edelbach, B. L.; Lachichotte, R. J.; Jones, W. D. *J. Am. Chem. Soc.* **1998**, *120*, 2843-2853. See also reference 12.

12) Konze, W. V.; Scott, B. L.; Kubas, G. J. *J. Am. Chem. Soc.* **2002**, *124*, 12550-12556.

13) Tellers, D. M.; Yung, C. M.; Arndtsen, B. A.; Adamson, D. R.; Bergman, R. G. *J. Am. Chem. Soc.* **2002**, *124*, 1400-1410.

14) a) Romeo, R.; Scolaro, L. M.; Pluntio, M. R.; Del Zotto, A. *Transition Met. Chem.* **1998**, *23*, 789-793. b) Alibrandi, G.; Bruno, G.; Lanza, S.; Minniti, D.; Romeo, R.; Tobe, M. L. *Inorg. Chem.* **1987**, *26*, 185-190.

15) Jutzi, P.; Müller, C.; Stammler, A.; Stammler, H.-G. *Organometallics* **2000**, *19*, 1442-1444.

16) Morris, G. A.; Freeman, R. *J. Magn. Res.* **1978**, *29*, 433-462.

17) Bain, A. D.; Cramer, J. A. *J. Magn. Res.* **1996**, *118*, 21-27.

18) Langford, C. H.; Gray, H. B. *Ligand Substitution Processes*; Benjamin: New York, **1966**; pp 18-54.

19) a) Romeo, R. *Comments Inorg. Chem.* **1990**, *11*, 21-57. b) Romeo, R.; Scolaro, L. M.; Nastasi, N.; Arena, G. *Inorg. Chem.* **1996**, *35*, 5087-5096. c) Romeo, R.; Alibrandi, G. *Inorg. Chem.* **1997**, *36*, 4822-4830. d) Romeo, R.; Plutino, M. R.; Elding, L. I. *Inorg. Chem.* **1997**, *36*, 5909-5916. e) Plutino, M. R.; Scolaro, L. M.; Romeo, R.; Grassi, A. *Inorg. Chem.* **2000**, *39*, 2712-2720.

20) Fernandez, A. L.; Wilson, M. R.; Prock, A.; Giering, W. P. *Organometallics* **2001**, *20*, 3429-3435.

21) Puddephatt, R. J. *Coord. Chem. Rev.* **2001**, *219-221*, 157-185.

22) For examples of 5-coordinate platinum(IV): a) Ulrich, F.; Kaminsky, W.; Goldberg, K. I. *J. Am. Chem. Soc.* **2001**, *123*, 6423-6424. b) Ulrich, F.; Goldberg, K. I. *J. Am. Chem. Soc.* **2002**, *124*, 6804-6805. c) Reinartz, S.; White, P. S.; Brookhart, M.; Templeton, J. L. *J. Am. Chem. Soc.* **2001**, *124*, 6425-6426. For lead references on 6-coordinate platinum(IV): d) Cotton, F. A.; Wilkinson, G.; Murillo, C. A.; Bochmann, M. *Advanced Inorganic Chemistry*, 6th ed.; John Wiley & Sons, Inc.: New York, 1999; pp 1080-1082. e) Roundhill, D. M. In *Comprehensive Coordination Chemistry*, Vol 5.; Wilkinson, G., Gillard, R. D., McCleverty, J. A., eds.; Peregemon Press: Oxford, 1987; pp 353-531.

23) Nozaki, K.; Sato, N.; Tonomura, Y.; Yasutomi, M.; Takaya, H.; Hiyama, T.; Matsubara, T.; Koga, N. *J. Am. Chem. Soc.* **1997**, *119*, 12779-12795.

24) We note that the 6-coordinate platinum(IV) complex $[PhBP_3]PtMe_3$ has been prepared and is thermally very robust. Thomas, J. C.; Peters, J. C. *Polyhedron* **2003**, 489-497.

25) Clark, H. C.; Manzer, L. E. *J. Organomet. Chem.* **1973,** *59*, 411-428.

26) Hackett, M.; Whitesides, G. M. *Organometallics* **1987**, *6*, 403-410.

27) Appleton, T. G.; Bennett, M. A. *Inorg. Chem.* **1978**, *17*, 738-747.

28) Schore, N. E.; Benner, L. S.; Labelle, B. E. *Inorg. Chem.* **1981**, *20*, 3200-3208.

29) Stehling, U. M.; Stein, K. M.; Kesti, M. R.; Waymouth, R. M. *Macromolecules* **1998**, *31*, 2019-2027.

30) LeSuer, R. J.; Geiger, W. E. *Angew. Chem., Int. Ed*. **2000**, *39*, 258-250.

31) Appleton, T. G.; Bennett, M. A.; Tomkins, I. B. *J. Chem. Soc., Dalton Trans.* **1976**, 439-446.

32) Smith, Jr., D. C.; Haar, C. M.; Stevens, E. D.; Nolan, S. P.; Marshall, W. J.; Moloy, K. G. *Organometallics* **2000**, *19*, 1427-1433.

33) Kemmitt, R. D. W.; Nichols, D. I.; Peacock, R. D. *J. Chem. Soc. (A)* **1968**, 2149-2152.

34) Bakshi, P. K.; Linden, A.; Vincent, B. R.; Roe, S. P.; Adhikesavalu, D.; Cameron, T. S.; Knop, O. *Can. J. Chem.* **1994**, 72, 1273-1293.